CHALMERS
UNIVERSITY OF TECHNOLOGY

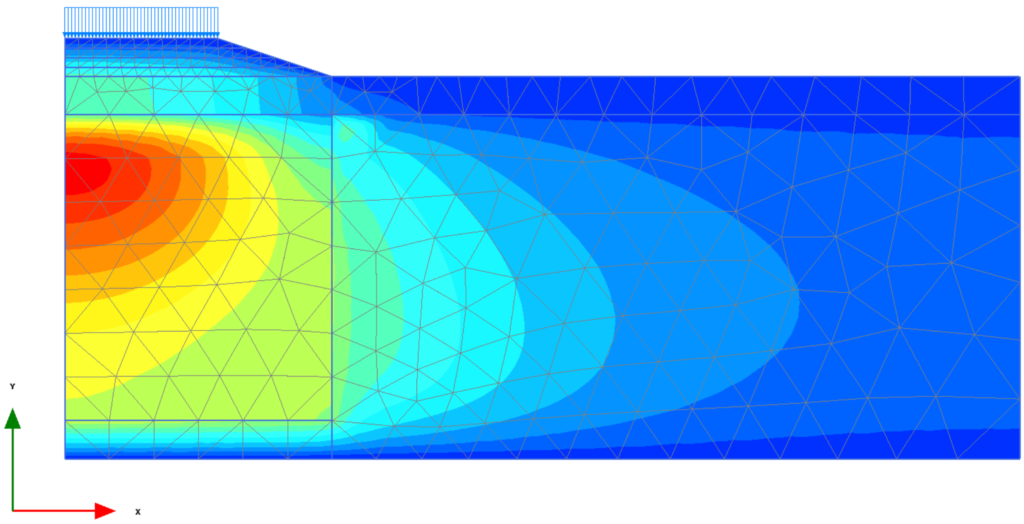

Numerical modelling of surcharge loading

Optimisation of surcharge loading to minimise long-term settlements in soft soil

Master's thesis in Infrastructure and Environmental Engineering

DARKO ASANOVIC
VALDRIN QYRA

Department of Architecture and Civil Engineering
CHALMERS UNIVERSITY OF TECHNOLOGY
Master's thesis 2017:85
Gothenburg, Sweden 2017

MASTER'S THESIS 2017:85

Numerical modelling of surcharge loading

Optimisation of surcharge loading to minimise long-term settlements in soft soil

DARKO ASANOVIC
VALDRIN QYRA

Department of Architecture and Civil Engineering
Division of Geology & Geotechnics
CHALMERS UNIVERSITY OF TECHNOLOGY
Master's thesis 2017:85
Gothenburg, Sweden 2017

Numerical modelling of surcharge loading
Optimisation of surcharge loading to minimise long-term settlements in soft soil
DARKO ASANOVIC
VALDRIN QYRA

Supervisor: Minna Karstunen, Department of Civil and Environmental Engineering
Examiner: Minna Karstunen, Department of Civil and Environmental Engineering

Master's Thesis 2017:85
Department of Architecture and Civil Engineering
Division of Geology & Geotechnics
Chalmers University of Technology
SE-412 96 Gothenburg
Telephone +46 31 772 1000

Cover: Visualisation of excess pore water pressure under ground improved embankment, constructed in Plaxis 2D.

Typeset in LaTeX
Gothenburg, Sweden 2017

Numerical modelling of surcharge loading
Optimisation of surcharge loading to minimise long-term settlements in soft soil
DARKO ASANOVIC
VALDRIN QYRA
Department of Architecture and Civil Engineering
Division of Geology & Geotechnics
Chalmers University of Technology

Abstract

The purpose of this study was to investigate if secondary compression in soft soils can be eliminated or minimised by optimisation of surcharge loading. The objective was to perform a numerical analysis of ground improvement with surcharge loading in combination with vertical drains, in order to find the optimal design. In this study an embankment was numerically modelled on a homogeneous soft soil layer representative for clay found in Utby, Gothenburg. The numerical modelling was performed in the software Plaxis 2D and Geosuite Settlement, where the models Creep-SCLAY1S and Chalmersmodel with creep was assessed respectively. The results are presented through the analysis of long-term settlements of the embankment. Simulations results shows significant differences between the two software. For Creep-SCLAY1S the creep rates could be improved, although the improvement starts to occur around 1300 years making it difficult to assess the method in practical applications. The simulations in Creep-SCLAY1S also revealed that no swelling occurred after unloading of surcharge. There is a suspicion regarding the model formulation in Creep-SCLAY1S, and this due to no swelling was identified and total settlements were in general excessive. In Geosuite Settlement the creep could be improved immediately after the unloading. In general, higher amount of surcharge did not prove to increase the creep improvement ratio in Geosuite. Although, higher amount of surcharge significantly improved the creep rates after unloading. It was also noted that the penetration depth of the drains could be reduced up to 40% in Creep-SCLAY1S without affecting the consolidation process. For Geosuite Settlement even small changes to the penetration length affected the consolidation process.

Keywords: Numerical modelling, Soft soil, Homogeneous soil, Embankment, Prefabricated vertical drains, Surcharge loading, Creep improvement ratio, Swelling, Creep-SCLAY1S, Geosuite Settlement.

Acknowledgements

Firstly we would like to to thank our supervisor and examiner Prof. Minna Karstunen, for her guidance and expertise throughout the work. We are extremely grateful for the opportunity to develop our knowledge in the field, and the opportunity to receive support and insights from the highly competent staff at the division of Geology & Geotechnics.

Secondly, we would like to thank the geotechnical staff at Norconsult AB who has provided us the practical knowledge concerning the software Geosuite Settlement. They have also showed great interest in our work and contributed with discussions that has widen our perspective of the subject.

Lastly, special regards goes out to both our families and friends that motivated and encouraged us on all levels in life, and shaped us to the individuals that we are today.

Darko Asanovic & Valdrin Qyra, Gothenburg, June 2017

Contents

List of Figures **x**

List of Tables **xii**

Nomenclature **xiii**

1 Introduction **1**
1.1 Background 1
1.2 Aim and objective 2
1.3 Limitations 2
1.4 Method 3

2 Theory **4**
2.1 Terzaghi's classical consolidation theory 4
2.2 Secondary compression of soft soil 5
2.3 Relation between secondary compression and overconsolidation ratio . 6
2.4 Surcharge loading 8
2.5 Prefabricated vertical drains 10
2.6 Geosuite Settlement 12
2.7 Creep-SCLAY1S 14
2.8 Embankment design 17

3 Method **18**
3.1 General information 18
3.2 Embankment and soil geometry 18
3.3 Simulations cases 19
3.4 Simulations with Geosuite Settlement 20
3.5 Simulation with Creep-SCLAY1S model 21

4 Results **24**
4.1 Simulation results from Geosuite Settlement 24
4.2 Simulation results from Creep-SCLAY1S 28

5 Conclusion **36**

Bibliography **38**

A Appendix **I**

A.1 Derivation of improved permeability (k_{eq}) I
A.2 Parameters needed for Chalmersmodel II
A.3 Denotation of creep number, r III
A.4 Parameters needed for Creep-SCLAY1S IV

List of Figures

1.1 Schematic outline of thesis. . . . 3

2.1 Illustration of differences in Hypothesis A and B (Fatahi et al., 2013). 6
2.2 Creep rate deviation with OCR for β-value 27 (Leoni et al., 2008). . . 7
2.3 The effects on soil when surcharge loading is used (Almeida and Marques, 2013). . . . 8
2.4 Effects of surcharging on the rate of secondary compression, Ladd (1971) presented in Conroy et al. (2015). . . . 9
2.5 Data collected from four different papers, results from Shannon Estuary, and Ladd's mean, upper and lower limit lines (Conroy et al., 2015). . . . 10
2.6 Schematic of the effects when combining surcharge load with and without vertical drains (Almeida and Marques, 2013). . . . 11
2.7 Illustration of the rheological model with combines phenomenas describing the long term deformations in the soil (Alén, 1998). . . . 12
2.8 Validation of Chalmersmodel with laboratory test results (Claesson, 2003). . . . 13
2.9 Relationship between creep number and vertical effective stress in Chalmersmodel. . . . 14
2.10 Illustration of the Creep-SCLAY1S model (Gras et al., 2015). . . . 15

3.1 Problem geometry, soil layers and generated mesh. . . . 19
3.2 Illustration of the three different cases simulated. . . . 20

4.1 Case II with unloading of AAOS after 2 year. Single drainage with PVDs at full penetration length. . . . 25
4.2 Case II with unloading of AAOS after 2 year. Double drainage with PVDs at full penetration length. . . . 25
4.3 Creep improvement ratio due to surcharge, derived from both drainage conditions in case II using the method proposed by Ladd (1971). . . . 26
4.4 Optimisation of penetration length of the PVDs for single drainage. . 27
4.5 Optimisation of penetration length of the PVDs for double drainage. 27
4.6 Results from case I, single- and double drainage conditions with and without PVDs. . . . 29
4.7 Case II with unloading of AAOS after 1 year. Single drainage with PVDs at full penetration length. . . . 30

4.8 Case II with unloading of AAOS after 1 year. Double drainage with PVDs at full penetration length. 30
4.9 Creep improvement ratio due to surcharge, derived from both drainage conditions in case II after 1300 years. 31
4.10 Horizontal displacements at embankment toe for different AAOS, case II for SD conditions. 32
4.11 Horizontal displacements at embankment toe for different AAOS, case II for DD conditions. 32
4.12 Optimisation of penetration length for single drainage. 33
4.13 Optimisation of penetration length for double drainage. 34
4.14 Horizontal displacements at embankment toe for single drainage when optimising penetration length of the PVDs. 35
4.15 Horizontal displacements at embankment toe for double drainage when optimising penetration length of the PVDs. 35

List of Tables

3.1 Parameters needed in Chalmersmodel with creep addendum. 21
3.2 Parameters needed for Creep-SCLAY1S-model used in Plaxis 2D. . . 22
3.3 Staged construction as loading for the embankment. 23

A.1 Calculation of improved permeability to represent the PVDs in the soil. I
A.2 Parameters needed for sand layer using Janbu-sand model. II
A.3 Model parameters the clay layer using Chalmersmodel with creep addendum. II
A.4 Calculated parameters for Chalmersmodel with creep addendum. . . . III
A.5 The additional initial stress state parameters for the soil layers. . . . IV
A.6 Isotropic parameters used for the clay layer. IV
A.7 Anisotropic parameters used for the clay layer. IV
A.8 Destructuration parameters used for the clay layer. IV
A.9 Viscous parameters used for the clay layer. IV

Nomenclature

Abbrevations

$AAOS$	Adjusted Amount of Surcharge
CC	Center to Center
CL	Center Line
CSR	Constant Rate of Strain
CSS	Current Stress State
DD	Double Drainage
EOP	End of Primary Consoldation
IL	Incremental Loading
NCS	Normally Consolidated Surface
OCR	Overconsolidation ratio
POP	Pre Overburden Pressure
PVD	Prefabricated Vertical Drains
SD	Single Drainage
U	Degree of Consolidation

Greek Symbols

α	Adhesion factor
α_0	Initial value of α
α_d	Deviatoric fabric tensor
β	Creep exponent
χ	Degree of bonding
χ_0	Initial value of χ
$\delta*$	Modified compression index
δ^*	Modified compression index
ϵ_d^p	Plastic deviatoric strain
ϵ_v^p	Plastic volumetric strain
η	Stress ratio

η_0	Initial stress ratio
γ	Unit weight of soil
γ_w	Unit weight of water$[kN/m^3]$
γ_{emb}	Unit weight of embankment
κ	Slope of recompression curve
$\kappa*$	Modified swelling index
Λ	Visco-plastic multiplier
μ^*	Modified creep index
μ_i^*	Modified intrinsic creep index
ω	Absolute rate of rotation of yield surface
ω_d	Relative effectiveness of plastic strain
σ'	Effective stress $[kPa]$
σ'_p	Pre-consoldiation pressure $[kPa]$
σ'_{vf}	Final effective stress $[kPa]$
σ'_{vs}	Effective stress under surcharge
τ	Reference Time
ξ	Absolute rate of destructuration
ξ_d	Relative effectiveness of destructuration rate

Roman Symbols

$\dot{e}$	Rate of change of void ratio
$\dot{e}^e$	Elastic rate of change of void ratio
$\overline{U}_h$	Average degree of horizontal consolidation
a_0	Stress factor
a_1	Stress factor
b_1	Stress factor
b_o	Stress factor
C_α	Secondary compression index
C_c	Compression index
C_h	Coefficient of consolidation in horizontal direction $[m^2/year]$
C_s	Swelling index
c_v	Coefficient of vertical consolidation $[m^2/year]$
d_e	Equivalent drainange diamater $[m]$
d_w	Diameter of drain
e^c	Rate of change of voids due to creep

H	Thickness $[m]$
h_f	Height of embankment $[m]$
h_{fs}	Height of surcharge $[m]$
k	Hydraulic conductivity $[m/s]$
k_h	Hydraulic conductivity in horizontal direction $[m/s]$
k_s	Hydraulic conductivity in smear zone $[m/s]$
l	Drainage length $[m]$
M	Compression modulus $[kPa]$
M'	Stress-dependent component modulus for stress $\geq \sigma'_L$
M_L	Component modulus between pre-consolidated pressure and σ'_L
M_o	Component modulus in over-consolidated state
p'	Mean effective stress $[kPa]$
p'_p	Size of normal consolidation surface in p'-q plane $[kPa]$
p'_{eq}	Size of current stress surface in p'-q plane $[kPa]$
p'_{mi}	Size of intrinsic yield curve in p'-q plane $[kPa]$
p_0	In-situ effective mean stress $[kPa]$
q_w	Discharge capacity $[l/s]$
R	Time resistance
r	Creep number
t	Time
T_h	Time factor in horizontal direction
T_v	Time factor in vertical direction
u	Pore pressure $[kPa]$
z	Elevation head $[m]$

1

Introduction

This chapter provides a background to the study followed by the aim and objectives. Furthermore, the demarcations are specified and the method's section gives a brief description of how the study was performed. Lastly, this chapter presents the outline of the report.

1.1 Background

The urbanisation trend poses several construction challenges for engineers during the upcoming decades. More than half of the worlds population currently resides in urban areas (Kalmykova et al., 2015). By year 2050 an increase in population of 20-30% is expected in the urban areas worldwide. In order to meet this trend a large share of the urban development still needs to be constructed (Swillingand and Robinson, 2013). In synergy with the growing population in cities, line infrastructure connections between cities and other countries is crucial for establishing a sustainable and attractive transport system. Gothenburg city is the second largest city in Sweden that is currently undergoing major urbanisation. The city is located in the Western part of Sweden and has currently two large urban developments planned, Älvstaden and Västsvenska paketet (Mehner, 2017). Urban areas located in coastal regions are facing difficulties in locating good quality sites for new development. Gothenburg is one of the cities that is geologically located in a area dominated by soft soils. Generally, soft soils are prone to settlements and stability issues that geotechnical engineers will be facing in the near future.

The properties of soft soil is determined by various factors, type of deposition and geographic location of soil minerals has a large impact on the geotechnical characteristics. Glacial and postglacial clay deposits are common in the Nordic countries, Canada and Northern parts of the US. Soft soil deposits are often associated with low shear strength and high sensitivity, where the sensitivity can exceed 50. The volcanic clay deposits in Mexico City are characterised by the high water content and are highly compressible with large secondary compression. The Bangkok clay is generally uniform although intersection by fine cracks are present. The sensitivity is low and the compressibility of the clay is high (Knappett and Craig, 2012). In short, the characteristics of the soft soils deposits varies by location and should be analysed separately for detailed information regarding soil properties.

Kansai International Airport is one example of a project initiated where new land has been reclaimed. The project comprises of two islands, island I and II, located in Osaka Bay (Japan). The project has received large attention in geotechnical papers due to its large scale and complexity. Both island I and II are continuously settling, predictions indicate that both will be under sea level by end of the this century (Mesri and Funk, 2015). The difficulties with these large scale projects is usually the settlement predictions. Site investigations and laboratory consolidation tests has not proven to be give enough information for the settlement predictions. Secondary compression can also contribute significantly to the settlements even during the primary consolidation, although at end of the primary consolidation process secondary compression is more evident (Puzrin et al., 2010).

Due to the complexity of fully understanding soft soil behaviour, researchers has proposed several constitutive models in order to receive more accurate settlement and stability predictions. One of the most recently proposed models is Creep-SCLAY1S, a model developed to predict the long-term settlements in soft sensitive clays. In addition to the isotropic parameters, the model also takes into account the anisotropy, destructuration and viscosity of the soft soil. Numerical modelling enables advanced embankment designs to be analysed. The embankment will be modelled in Plaxis 2D (using Creep-SCLAY1S as a model) and the commercial software Geosuite.

1.2 Aim and objective

The aim of this thesis is to investigate if secondary compression in soft soils can be eliminated or minimised by optimisation of surcharge loading. The objective is to perform a numerical analysis of ground improvement with surcharge loading in combination with vertical drains, in order to find the optimal design.

1.3 Limitations

In this thesis a homogeneous clay layer has been analysed. The soil parameters are based on the Utby clay and has earlier been derived and evaluated at Chalmers University of Technology. The selected ground improvement methods are less common in the Scandinavian countries and was particularly chosen for that reason.

1.4 Method

After the problem identification the investigation proceeded with a literature review regarding surcharge loading, vertical drains and numerical modelling. Further on, a review of the Creep-SCLAY1S model and Geosuite Settlement was done in order to understand how the models works and what parameters are included. After the literature study was completed, a set of parameters was chosen to perform the simulations in the numerical tools. Three different cases was set to realise the aim of the thesis, where several simulations was made to find the optimal solution of surcharge load and penetration depth of the drains. In the last part of this study an analysis of the results and conclusion was conducted. Figure 1.1 schematically summarises the structure of this paper.

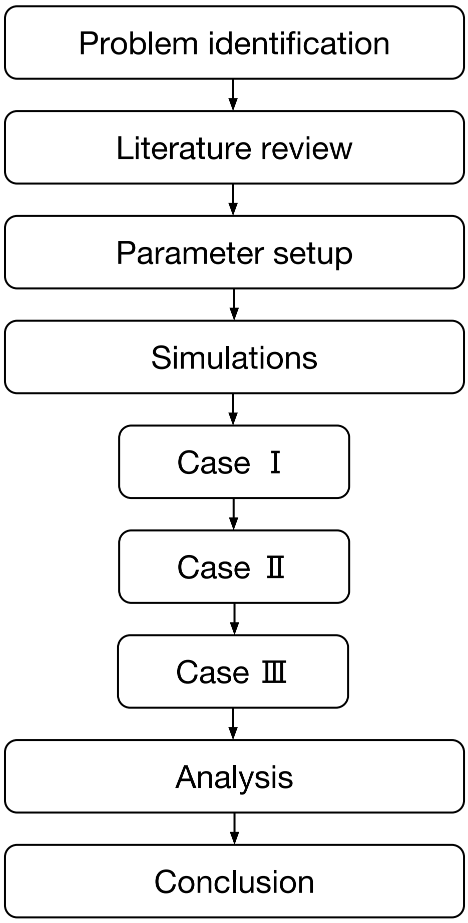

Figure 1.1: Schematic outline of thesis.

2

Theory

In the following sections, relevant literature and knowledge that concerns the master thesis is presented. Initially the consolidation theory of soft soils is presented, followed by the relevant ground improvement methods used in the thesis. Lastly, the theory for the constitutive models are presented.

2.1 Terzaghi's classical consolidation theory

Primary consolidation is a time-dependent volumetric deformation of soils with low permeability. This occurs due to application of a load on the surface (i.e. change in effective stress), which immediately results in an increase of pore water pressure and build up of excess pore water pressure in the soil. As a result, the hydraulic gradient increases and as a consequence drainage of the pore water in the soil occurs, until the equilibrium is reached, with deformations keep developing in the soil (Knappett and Craig, 2012). The mathematical formulation for calculating the degree of consolidation at any time t, was developed by Terzaghi (1943). The theory is valid for one-dimensional consolidation calculations and is widely accepted. The Equation 2.1 presents the formulation.

$$T_v = \frac{c_v}{H^2} \cdot k \tag{2.1}$$

where the T_v is the time factor in vertical direction, H is the thickness of the soil layer [m], k is the hydraulic conductivity $[m/s]$. The coefficient of consolidation in vertical direction, c_v $[m^2/s]$, is expressed as Equation 2.2.

$$c_v = \frac{k \cdot M}{\gamma_w} \tag{2.2}$$

where M represents the compression modulus $[kPa]$ and γ_w is the unit weight of the water $[kN/m^3]$.

The classical consolidation theory proposed by Terzaghi (1923) relies on the unique relationship between effective stress and time independent strain. Additionally, the modulus and the permeability of the soil is assumed to be constant with time.

Equations 2.3 & 2.4 presents the theory in two different formats,

$$\frac{\partial u}{\partial t} = \frac{M}{\gamma}\frac{\partial}{\partial z}\left(k \cdot \frac{\partial u}{\partial z}\right) \qquad or \tag{2.3}$$

$$\frac{\partial u}{\partial t} = c_v \frac{\partial^2 u}{\partial z^2} \tag{2.4}$$

Equation 2.4 is based on several assumptions where the first assumes fully saturated and homogeneous soil. The strain and pore water flow is assumed to be one-dimensional and Darcy´s law is valid. The change in pore water pressure is equal to the change in effective stress, the equation also assumes that the pore water and soil particles are incompressible. The last assumption is that the strain is strictly dependent on the effective stress.

2.2 Secondary compression of soft soil

Secondary compression, also known as creep, is generally studied via from one dimensional consolidation tests conducted in the laboratory. The laboratory tests is usually presented in a time-compression curve where initial and primary consolidation can be obtained. The initial compression occurs due to a load is applied to the soil and immediate settlements are detected. As mentioned, primary consolidation occurs due to dissipation of excess pore water pressure and is therefore the driving force that causes the settlements. In contrast, a clear definition of secondary compression is yet not established and creep is still a challenge in geotechnical engineering. However, different theories has been presented to resolve the advancement of creep in soft soils.

One of the theories refer to the micro- and macro-fabric of the soft soils. Observations of the anisotropic fabric of soft soils shows low internal porosity for the clay minerals (Navarro and Alonso, 2001). The range of the porosity varies within 10-100 *nm* where water could be in a adsorbed state. The amount of adsorbed water is determined by the specific surface of the soil particles and is called microstructural water. The microstructural water has different properties from the free water in clay minerals when considering the aspects of structure and thermodynamics. The concept of this theory is to analyse the local water transfer from the mictrostructural voids to the macrostructurals voids of the soft soil body. Therefore, understanding changes in volume over time in the microscale can provide knowledge of deformations in the macroscale. However, until this equilibrium is reached, the long-term creep deformation are continuously occurring (Navarro and Alonso, 2001). Other theories propose that creep to be dependent on various factors where chemical, geomicrobiological and mechanical processes has great effect (Mitchell and Soga, 2005).

Further implications follows when determining creep in practical applications, as in determining the long-term settlements. These implications exists since disagreement among researchers regarding when creep starts to occur in the consolidation process. In the late 1970s, a theory was developed by Ladd et al. (1977) describing two creep hypothesis, A and B. In hypothesis A, it is claimed that creep starts after the end of primary consolidation (EOP), i.e after dissipation of excess pore water pressure. Hypothesis B refer to that primary and secondary compression are dependent, thus creep occurs simultaneously with primary consolidation. Currently, Hypothesis B is most accepted in geotechnical engineering. The Figure 2.1 illustrates the differences for Hypothesis A and B, with same initial conditions and effective stresses ($\Delta p/p_o$) (Fatahi et al., 2013).

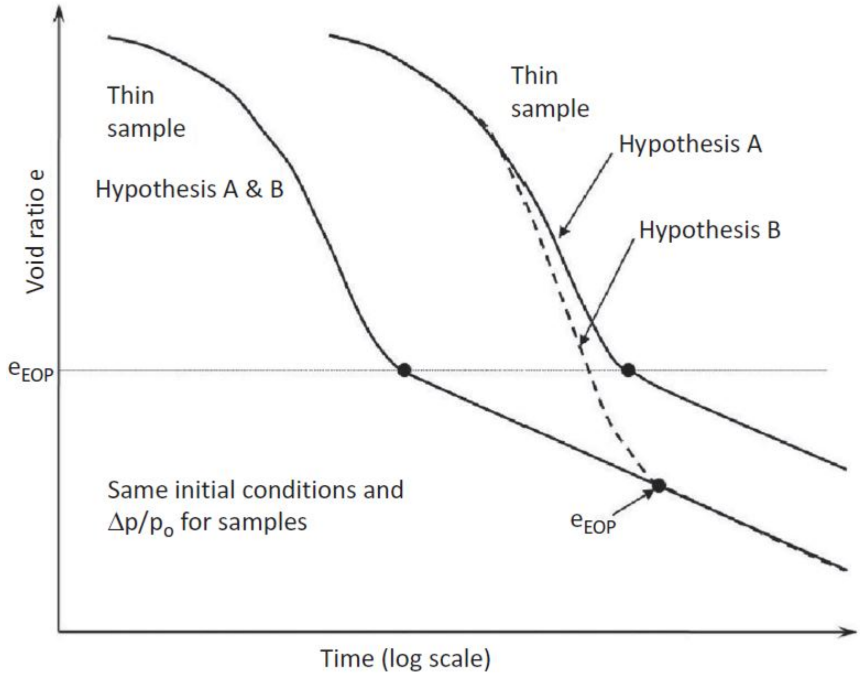

Figure 2.1: Illustration of differences in Hypothesis A and B (Fatahi et al., 2013).

2.3 Relation between secondary compression and overconsolidation ratio

The basic elasto-plastic theory implies an assumption of dividing the deformation in elastic and plastic strain components. The elastic part is observed due to an immediate settlement of the soil when a load is subjected to it, whereas the plastic component is time dependent (Leoni et al., 2008). Equation 2.5 illustrates the components in terms of void ratios where the superscripts e and c means elastic and creep components, respectively.

$$\dot{e} = \dot{e}^e + \dot{e}^c \tag{2.5}$$

The elastic component in Equation 2.5 describes the change of void ratio in the soil. C_s describes the swelling index and σ' is the effective stress in the soil. The dot in seen in $\dot{e}^e$ and $\dot{\sigma}$ notes the equation is time-dependent. The negative sign in Equation 2.6 follows from the conventional signs in soil mechanics where compression is positive.

$$\dot{e}^e = -\frac{C_s}{\ln 10}\frac{\dot{\sigma}'}{\sigma'} \tag{2.6}$$

The plastic component is due to the viscous behaviour of soft soil, and therefore the deformations are time-dependent. Equation 2.7, also referred as the power law, illustrates the phenomena where C_α and C_c are the secondary compression index and compression index, respectively, β is the creep exponent and τ is the reference time.

$$\dot{e}^c = -\frac{C_\alpha}{\tau \ln 10}\left(\frac{\sigma'}{\sigma'_p}\right)^\beta \qquad with \qquad \beta = \frac{C_c - C_s}{C_\alpha} \tag{2.7}$$

The ratio (σ'/σ'_p) is also referred as the inverse of the overconsolidated ratio (OCR). In Leoni et al. (2008), the relationship between creep rate and OCR with typical compression index values, which results into β=27, is demonstrated. In Figure 2.2 the void ratio is plotted against the effective stress with different OCR-values.

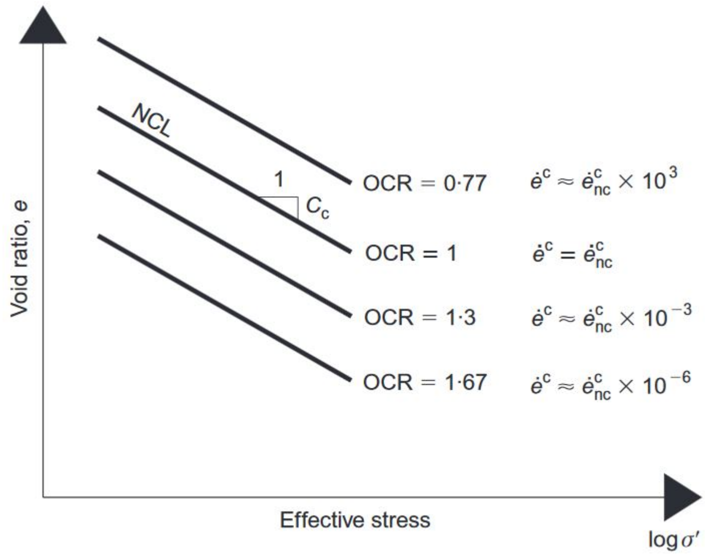

Figure 2.2: Creep rate deviation with OCR for β-value 27 (Leoni et al., 2008).

As seen in Figure 2.2, the creep rate is very high for the case of OCR less than one. Moreover, the creep rate is high for soils with OCR values around one and almost negligible for OCR higher than 1.3 (Leoni et al., 2008). This feature can potentially be exported in the design of surcharge loading in order to minimise or eliminate creep deformations.

2.4 Surcharge loading

Generally, there are two types of issues addressed when poor soil quality is encountered; stability and settlement problems. Therefore, different types of ground improvement techniques are used to control these issues and to strengthen the soil. There are methods available to improve both the stability and control settlements. It should be stressed that the soil properties at different locations should be analysed individually to find a suitable solution for ground improvement.

By applying a temporary surcharge load h_{fs} in excess of the final construction loads h_f the rate of settlement through primary consolidation is accelerated. Figure 2.3 shows the procedure in detail, where the total theoretical settlements (Δh_f) are achieved significantly faster with higher surcharge load at the equal time (t_1) (Almeida and Marques, 2013).

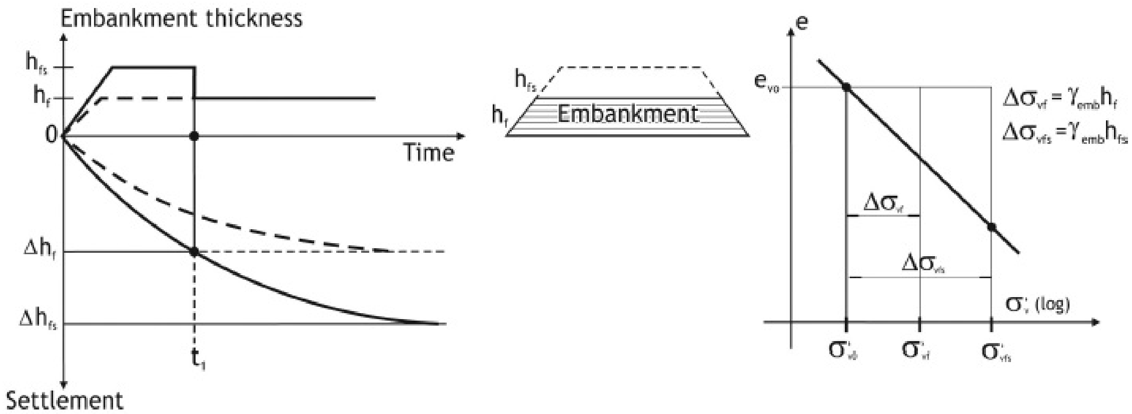

Figure 2.3: The effects on soil when surcharge loading is used (Almeida and Marques, 2013).

Unlike many other materials, soft soil experience significant volume changes under surcharge load. When unloading the surcharge and then reloading with the construction load, the goal is to minimise the change in volume. This to reduce the potential structural distresses in the future caused by the secondary compression in the soil (Tewatia et al., 2007). In Figure 2.3 shows that at time t_1 when the surcharge is removed, the settlement stabilisation rate is accelerated and thereby the secondary compression settlements are minimised. The removal of the surcharge can result in a rebound effect where the soil swells, however this phenomena is often neglected in the field (Almeida and Marques, 2013).

To achieve reduction in secondary compression by surcharge loading, the creep rate of C_α needs to be improved. As shown in Figure 2.4, this usually can be achieved after removal of the higher surcharge load. The soil swells for a certain duration after the surcharge has been removed. After the swelling ends the secondary compression resumes under a new constant effective stress. The secondary compression

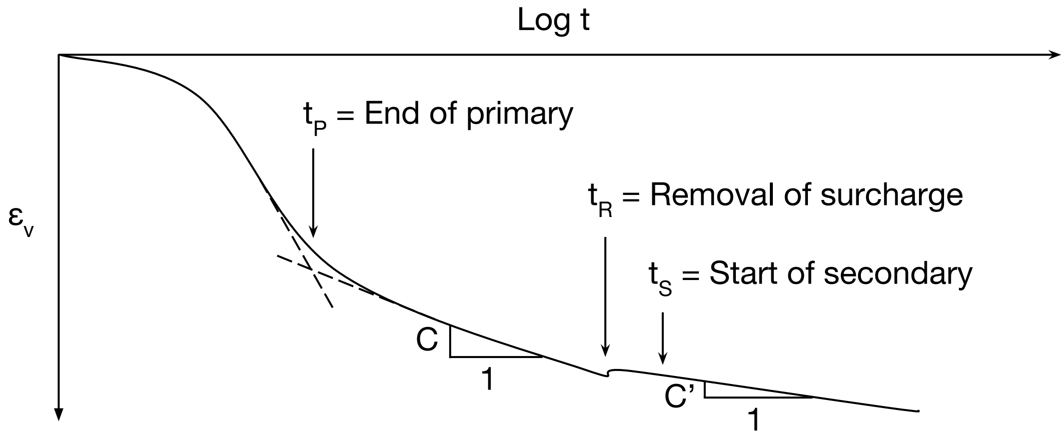

Figure 2.4: Effects of surcharging on the rate of secondary compression, Ladd (1971) presented in Conroy et al. (2015).

now occurs at a lower rate of C'_α than it would without surcharge loading. This behaviour proves that the longer time the surcharge loading is left in place, the more drawn-out time for swelling is needed before secondary compression with a lower compression rate continues C_α (Balasubramaniam et al., 2010). In the paper presented by Balasubramaniam et al. (2010) recommendations are given for the degree of consolidation (DOC) when preloading with and without PVDs. Generally, the DOC should be higher than 90% or even 95% in order to ensure that no primary settlements are added to the secondary settlements, and thus contributing to higher post-construction settlements.

Recent work by Conroy et al. (2015) has investigated the required amount of surcharge loading needed to improve the rate of secondary compression. The analysis was based on the procedure of long term oedometer tests at various levels of surcharge loading. The paper concluded that Ladd's method, as cited in Conroy et al. (2015) may be used as a good estimate in design of embankments on soft soils. In Equation 2.8 the adjusted amount of surcharge can be calculated, where σ'_{vs} is the effective stress under surcharge, and σ'_{vf} is the final effective stress after the surcharge loading has been removed. Ladd (1971) discovered that the ratio of C'_α to C_α is related to the level of surcharge loading applied to the soil. The relationship between C'_α/C_α and the adjusted amount of surcharge, (AAOS) is presented in Figure 2.5. As can be seen, higher amount of AAOS gives better creep improvement ratios.

$$AAOS = \frac{\sigma'_{vs} - \sigma'_{vf}}{\sigma'_{vf}} \tag{2.8}$$

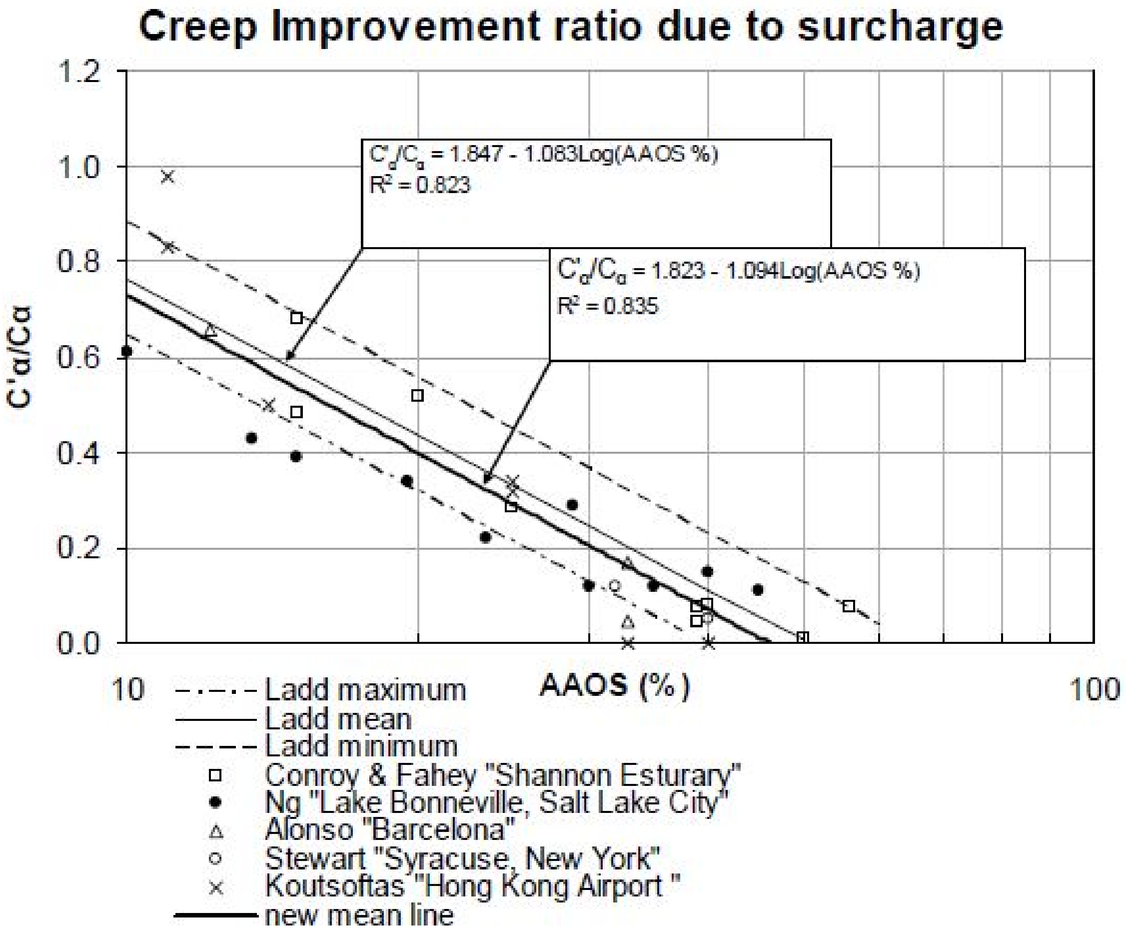

Figure 2.5: Data collected from four different papers, results from Shannon Estuary, and Ladd's mean, upper and lower limit lines (Conroy et al., 2015).

2.5 Prefabricated vertical drains

Soft soils have a slow rate of consolidation due to the low permeability. This can be accelerated by installing prefabricated vertical drains (PVDs) in the soil. The theory of vertical drains is to reduce the drainage path and in that way increase the rate of consolidation, resulting into faster dissipation of pore water pressure (Knappett and Craig, 2012). The PVDs have limited stiffness, thus installation in the soil should be done carefully. If the drain buckles during installation the drainage effectiveness is significantly reduced. Combined with the PVDs, a drainage blanket made of sand is usually constructed on top of the drains. The purpose of the blanket is to remove the water delivered from the drains away from the embankment construction. The drainage blanket should have an adequate thickness and inclination to enable discharge of the water by gravity. However, discharging the water could also be done by installing a pump attached to the drainage blanket (Almeida and Marques, 2013).

The theory of calculating the average degree of horizontal consolidation $\overline{U_h}$ in practical applications with drains was introduced by Hansbo (1981). The formula assumes equal vertical strain and does not consider the vertical drainage of the natural soil. The last assumption may give unrealistic results for thin soft soil layers with drainage layers both on top and bottom (Kirsch and Bell, 2013). It can be calculated at a depth, z, and at time, t, from 2.9,

$$\overline{U_h} = 1 - \exp\left(- \frac{8T_h}{\mu} \right) \tag{2.9}$$

where T_h is the time factor for horizontal consolidation and μ is accounting for both the smear and well resistance in the drain. The equations for T_h and μ are presented as:

$$T_h = \frac{c_h t}{d_e^2}, \tag{2.10}$$

$$\mu = \ln\frac{n}{s} + \frac{k_h}{k_s}\ln(s) - \frac{3}{4} + \pi\frac{2l^2 k_h}{3q_w} \tag{2.11}$$

where c_h represents the coefficient of consolidation in horizontal direction, d_e represents the equivalent drainage diameter of the drain dependent on the c-c distance, and t is equal to time presented in Equation 2.10. In Equation 2.11, $n = \frac{d_e}{d_w}$, where d_w is the diameter of the drain, $s = \frac{d_s}{d_w}$ where d_s is the diameter of the smear zone. The hydraulic conductivity values, k_h and k_s, shows the conductivity of the soil in horizontal plane and the smear zone respectively. The l parameter determines the drainage length and q_w determines the discharge capacity of the vertical drains. The first part of the equation, including the constant $-\frac{3}{4}$, accounts for the smear zone, whereas the second part presents the well resistance in the drain (Chai et al., 2001). In general the PVDs are combined with surcharge load to increase the rate of settlements in the natural subsoil. In some cases where the soft soil profile is thick with low permeability, it is reasonable to use the combination of the two soil improvement methods (Brand and Brenner, 1981). In Figure 2.6 the enhanced efficiency of the vertical drains are schematically illustrated, proving that settlements occur at a faster pace.

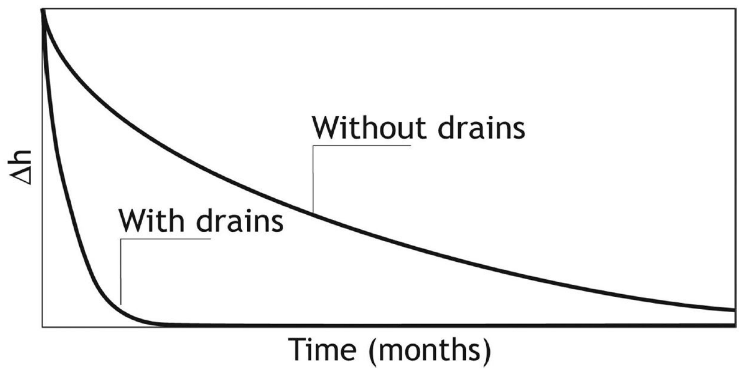

Figure 2.6: Schematic of the effects when combining surcharge load with and without vertical drains (Almeida and Marques, 2013).

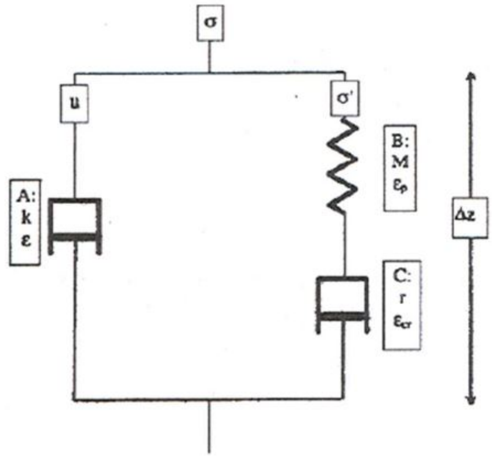

Figure 2.7: Illustration of the rheological model with combines phenomenas describing the long term deformations in the soil (Alén, 1998).

2.6 Geosuite Settlement

The finite element engine used in Geosuite Settlement is based on the rheological model proposed by Alén (1998). The theory of the model is based on the classical one-dimensional consolidation theory presented by Terzaghi (1923). Moreover, development and validation of the Chalmersmodel implemented in Geosuite have been done when analysing creep in the soft soils. This simple model is governed by the three phenomena; consolidation (A), elastic and plastic deformation (B) and creep deformation (C). The consolidation process accounts for the pore water dissipation and also restricts the strain rate. Elastic and plastic strains in the soil are detected by the model due to an increase of effective stress and the creep strain is occurring due to a constant effective stress level over time. The Figure 2.7 below illustrates the model with the different phenomenas. The combined effects of the three phenomena on soil, considering the deformations with time, can be derived from Equation 2.12.

$$\frac{\partial \epsilon_z}{\partial t} = -\frac{1}{M} \cdot \frac{\partial u}{\partial t} + \frac{1}{R} \tag{2.12}$$

where M is the oedometer modulus of the soil, u is the pore water pressure, t represents the time and R is the time resistance.

When considering the change in pore water pressure over time ($\partial u/\partial t$) similar equation proposed in Terzaghis consolidations theory can be used, except from the creep addendum. In Equation 2.13 the change in pore pressure with respect to time is presented.

$$\frac{\partial u}{\partial t} = \frac{M \cdot k_z}{\gamma_w} \frac{\partial^2 u}{\partial z^2} + \frac{1}{R} \tag{2.13}$$

where γ_w represents the unit weight of the water, k the permeability at different depth and the creep addendum is the ratio $1/R$.

The settlements parameters in Geosuite Settlement are based on three compression

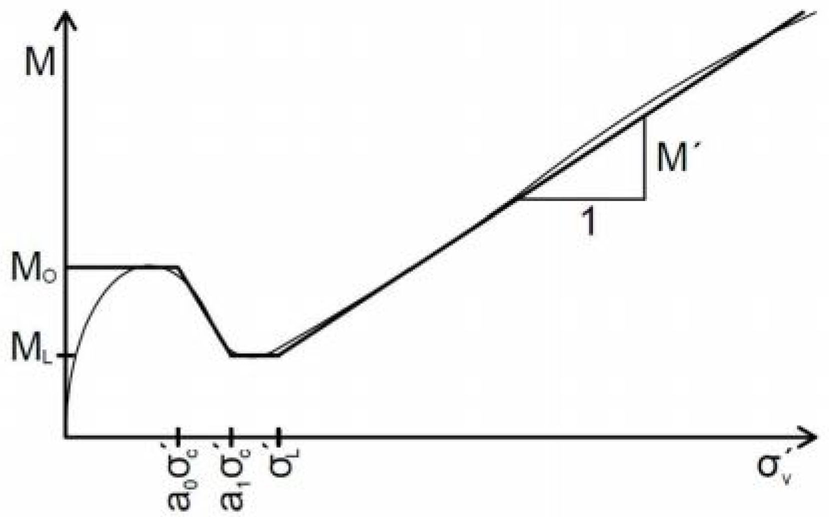

Figure 2.8: Validation of Chalmersmodel with laboratory test results (Claesson, 2003).

resistance modulus; M_o, M_L and M'. These parameters are derived from constant rate of strain oedometer tests. Moreover, the results are validated in the manner that the $\sigma' - M$-diagram shown in figure 2.8 matches the CRS laboratory tests (Swedish Standard Institute, 1991). According to Claesson (2003), this method is more suitable than the older Swedish practice when doing settlement calculations in soft soil. This due to that the Chalmersmodel does an adaption of the oedometer modules around the preconsolidation pressure from M_0 to M_L. This phenomena could be seen in Figure 2.8.

Further on, the stress factors a_o and a_1 could be set as 0.8 and 1.0 respectively. In order to calculate the oedometer modules, M, around the preconsolidation pressure, empirical formula's have been denoted and they are illustrated in Equation 2.14.

$$M = \begin{cases} M_0 & \text{if} \quad \sigma'_v < a_0\sigma'_c \\ M_0 + (M_L - M_0)\frac{\sigma'_v - a_0\sigma'_c}{a_1\sigma'_c - a_0\sigma'_c} & \text{if} \quad a_0\sigma'_c \leq \sigma'_v < a_1\sigma'_c \\ M_L & \text{if} \quad a_1\sigma'_c \leq \sigma'_v < \sigma'_L \\ M_L + M'(\sigma'_v - \sigma'_L) & \text{if} \quad \sigma'_v \geq \sigma'_L \end{cases} \tag{2.14}$$

Additionally, an extension was made to take the creep factor into account. When considering the creep supplement, five more parameters are needed to calculate the time resistance R, which could be found in Equation 2.13. Similar to the oedometer modules, Claesson (2003) claims that the creep number, r_s, is a better estimation when considering the creep behaviour of soft soil than secondary coefficient of consolidation, C_α. In Chalmersmodel, the creep number is denoted from the four remaining parameters r_0, r_1, b_0 and b_1. The stress parameter b_1 could be set to either 1.0 or 1.1, although the most common value is 1.1. In Figure 2.9, the creep number is described according to Chalmersmodel and how it is calculated based on

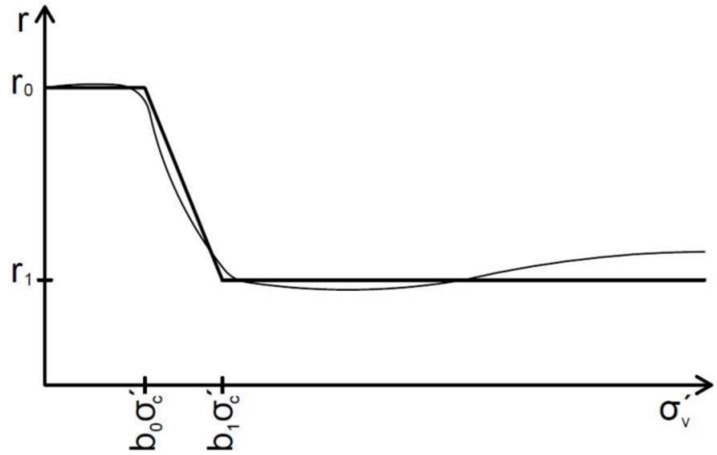

Figure 2.9: Relationship between creep number and vertical effective stress in Chalmersmodel.

the stress state the soil is in. The bold line describes the theoretical relationship between whereas the second line is simulated with Chalmersmodel.

In addition to the graph, empirical formula's are used to denote the creep number as seen in Equation 2.15.

$$r = \begin{cases} r_0 & \text{if} \quad \sigma'_v \leq b_0\sigma'_c \\ r_0 + (r_1 - r_0)\frac{\sigma'_v - b_0\sigma'_c}{b_1\sigma'_c - b_0\sigma'_c} & \text{if} \quad b_0\sigma'_c < \sigma'_v < b_1\sigma'_c \\ r_1 & \text{if} \quad \sigma'_v \geq b_1\sigma'_L \end{cases} \tag{2.15}$$

In Appendix A.2 and A.3, a table of the parameters needed for Chalmersmodel with the creep addendum and equations needed to denote the parameters respectively.

2.7 Creep-SCLAY1S

The most recent developed models in geotechnical engineering accounts for the anisotropic behaviour in soft soils. These models has proven to be more accurate compared to earlier ones which only assumed isotropic behaviour. Isotropic elasto-plastic soil models, not accounting for anisotropy has proved to be highly inaccurate in prediction of the soil response under loading (Wheeler et al., 2003). Some of the anisotropic models available are S-CLAY1, S-CLAY1S and Multilaminate Model for Clay (MCC).

The Creep-SCLAY1S model is an extension of the S-CLAY1S model. This model was developed in order to include initial bonding and destructuration in simulations of anisotropic soft soils. Creep-SCLAY1S is extended by the addition of a intrinsic surface together with a hardening law similar to the one in S-CLAY1S. The model completely represents the stress-strain behaviour of structured clays. It is

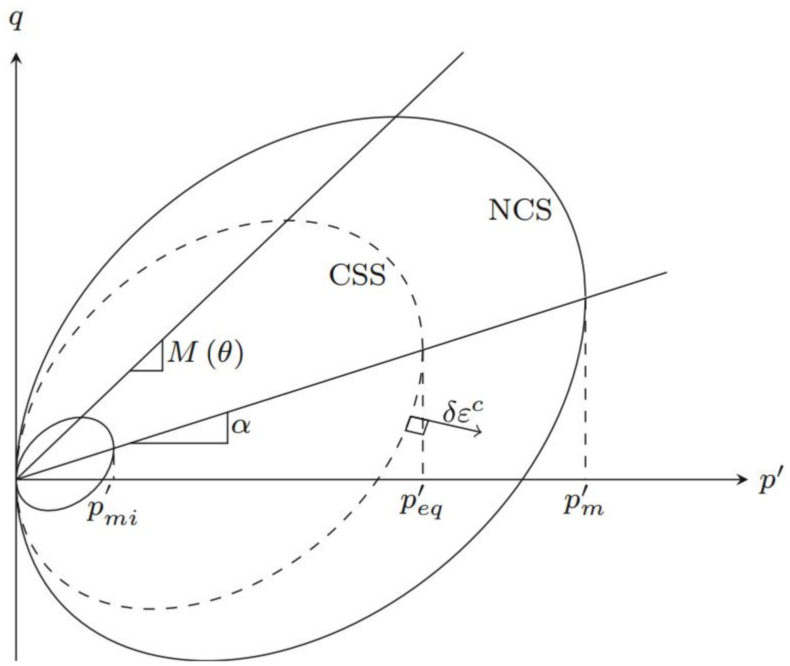

Figure 2.10: Illustration of the Creep-SCLAY1S model (Gras et al., 2015).

basically a rate dependent model that accounts for changes in fabric arrangement and bonding (Karstunen et al., 2013).

The intrinsic yield surface is denoted as p'_{mi}, Current Stress Surface (CSS) as p'_{eq} and Normal Consolidation Surface (NCS) as p'_p, and are illustrated in Figure 2.10. Equation 2.16 is referred as the volumetric hardening law and accounts for the evolution of the volumetric creep strains. The p'_p value specifies the size of Normal Consolidated Surface and is a boundary for the interval between the small and large creep strains. $\lambda_i^\star$ the modified compression index and $\kappa^\star$ the modified swelling index (Sivasithamparam et al., 2015).

$$\Delta p'_p = \frac{p'_p}{\lambda_i^\star - \kappa^\star} \Delta \epsilon_v^p \tag{2.16}$$

The inner ellipse specifies the Current Stress Surface and can be derived from Equation 2.17, where it represents the current state of the effective stress (Sivasithamparam et al., 2015).

$$p'_{eq} = \frac{p'^2 + (q - \alpha p')^2}{(M^2 - \alpha^2)p'} \tag{2.17}$$

Grimstad et al. (2010) presented the visco-plastic multiplier which accounts for creep behaviour in soft soils. The multiplier is presented in Equation 2.18 where $\mu_i^\star$ is the intrinsic creep index and is usually derived from IL oedometer tests. Although, the term $(M_c^2 - \alpha_0^2)/(M_c^2 - \eta_0^2)$ is added to the equation to provide correct creep strains with the corresponding measured volumetric creep strain rate under Oedometer conditions (Sivasithamparam et al., 2015).

$$\dot{\Lambda} = \frac{\mu_i^\star}{\tau}\left(\frac{p^{eq}}{(1+\chi)p'_{mi}}\right)^{\frac{\lambda_i^\star-\kappa^\star}{\mu_i^\star}}\frac{M_c^2-\alpha_0^2}{M_c^2-\eta_0^2} \tag{2.18}$$

The M_c-value which denotes the critical state slope can be derived from triaxial compression tests. The parameters α_0 and η_0 refers to the initial inclination of the yield surface and stress ratio corresponding to K_O Consolidation, respectively. Including the visco-plastic multiplier the analysis can extend above the critical state line and enter the dry side similarly to the MCC model. For overconsolidated soils this can in many cases result in a higher undrained shear strength. An associated flow rule is assumed in the Creep-SCLAY1S model where creep strain rate is defined by the visco-plastic multiplier shown in Equation 2.19.

$$\epsilon_{ij}^{\dot{c}} = \dot{\Lambda}\frac{\partial p'_{eq}}{\partial \sigma'_{ij}} \tag{2.19}$$

The hardening laws similar to the S-CLAY1S model are as mentioned included in the model, with the plastic strains are exchanged with creep strains. The first hardening law represents the increased size of the intrinsic yield surface p'_{mi} seen in Equation 2.20.

$$\dot{p}'_{mi} = \frac{vp'_{mi}}{\lambda_i - \kappa}\dot{\epsilon}_v^c \tag{2.20}$$

Although, the first hardening law in Equation 2.20 can be reduced to MCC-analysis from Equation 2.16 if destructuration is ignored. The second hardening law was presented by Wheeler et al. (2003) and is presented in Equation 2.21. The hardening law describes the change in the orientation of the yield surface, also known as the rotational hardening law.

$$\dot{\alpha}_d = \omega\left[\left(\frac{3\eta}{4}-\alpha_d\right)\left\langle\dot{\epsilon}_v^c\right\rangle + \omega_d\left(\frac{\eta}{3}-\alpha_d\right)\dot{\epsilon}_d^c\right] \tag{2.21}$$

In the equation, η represents the stress ratio, ω and ω_d are model constants. ω determines the absolute rate of rotation of the yield surface, and ω_d controls the relative effectiveness of plastic strains. The third hardening law considers the degradation of inter-particle bonding with plastic straining. The bonding parameter χ is introduced and gets reduced to zero with an increase in plastic strains. Change in bonding χ can be derived from Equation 2.22.

$$d\dot{\chi} = \xi[(0-\chi)|\dot{\varepsilon}_v^c| + \xi_d(0-\chi)\dot{\varepsilon}_d^c] = -\xi\chi(|\dot{\varepsilon}_v^c| + \xi_d\dot{d}_d^c) \tag{2.22}$$

The bonding paramter χ is dependent of the two soil properties, ε and ε_d which governs the absolute rate of destructuration and relative effectiveness of plastic strains during bond degradation. In Creep-SCLAY1S the critical state M is included as a function of a lode angle. The function for the critical state is given by Equation 2.23, m represents the ratio between critical state slope in extension and the critical state in compression.

$$M(\theta) = M_c\Big(\frac{2m^4}{1+m^4+(1-m^4)\sin 3\theta_\alpha}\Big)^{\frac{1}{4}} \tag{2.23}$$

2.8 Embankment design

The typical embankments constructed is Sweden are based on the guidelines pursuant to the Transport Administration (Trafikverket). Embankments should be built in the manner that no nearby construction is affected. Additionally, no compromises should be taken which could impact the stability of the construction or the embankment. If there is risk for environmental impact, embankments should be constructed according to different categories described in Alm (2000).

The standardised road widths in Sweden for a $2+2$ highway, can be designed based on document Alm (2000). The following dimensions are assumed for the road width in one direction, two lanes is equal to 7.5 meters, one verge of 3 meters, two outer hard strip edges of 0.5 meters. Summarising these, a total crown width should at least be 11 meters.

Slopes in Sweden are usually 1:3, these slopes puts drivers at risk for overturning. Flatter slopes has been recommended, 1:4 to 1:6, and even flatter can reduces the risk of overturning significantly. High embankment heights can be built with both steeper or flatter inclinations depending on how much space can be allocated for the road (Alm, 2000).

3

Method

The third chapter is concerned with the methodology for this study. All relevant information regarding how the analysis was performed can be found in this chapter. Simulations was done in Geosuite Settlement and Plaxis 2D, where access was given to the yet commercially unavailable Creep-SCLAY1S model.

3.1 General information

The idealised embankment was analysed on Utby clay and is located in the outskirts of Gothenburg. In general, the Utby clay shows similar characteristics with the soft soils found in the Gothenburg region. Researchers at Chalmers University of Technology are currently using the Utby site for soil testing. The available laboratory tests for the Utby clay are Odeometer tests, both incremental loading (IL) and constant rate of strain (CRS), and triaxial tests. The laboratory tests have been conducted from mini-block samples and piston samples and validation of the parameters have been done for both types by Karlsson et al. (2016). In this thesis, data for the two models used have been derived from the same IL tests extracted at eight meters depth. The soil under the embankment was improved with prefabricated vertical drains. The drains are assumed to be 100 mm wide and 4 mm thick. The arrangement of the prefabricated vertical drains was set to a square pattern with 2 m of centre-to-centre distance. To represent the PVDs in the clay, improvement of permeability accordingly to Chai et al. (2001) has been performed. The improvement of permeability is a simplification to assess PVDs in 1D- and 2D-analysis. In Appendix A.1 the calculations are presented. On top of the embankment surcharge loading was applied to increase the rate of primary consolidation, and thus increase the undrained shear strength and minimise creep.

3.2 Embankment and soil geometry

The embankment was symmetric and therefore only the right half was analysed. The dimensions of the embankment was 14 meters wide, 2 meters high and it was constructed on a 2 meters thick dry crust layer. Under the dry crust layer, a 18 meters thick clay layer followed. Although, when vertical drains was assessed in the analysis, a sand layer with a thickness of 2 meters and a width of 14 meters had to be included in the model. The sand layer works as a drainage layer and supports the drains to numerically reach the true drainage capacity. Furthermore, the groundwater table was set at 2 meters below the surface. Slope inclinations was set to 1:3 meters which is the most common practise in Sweden. In Figure 3.1 the finite element model dimensions are shown, where the depth was 20 meters and 50 meters wide.

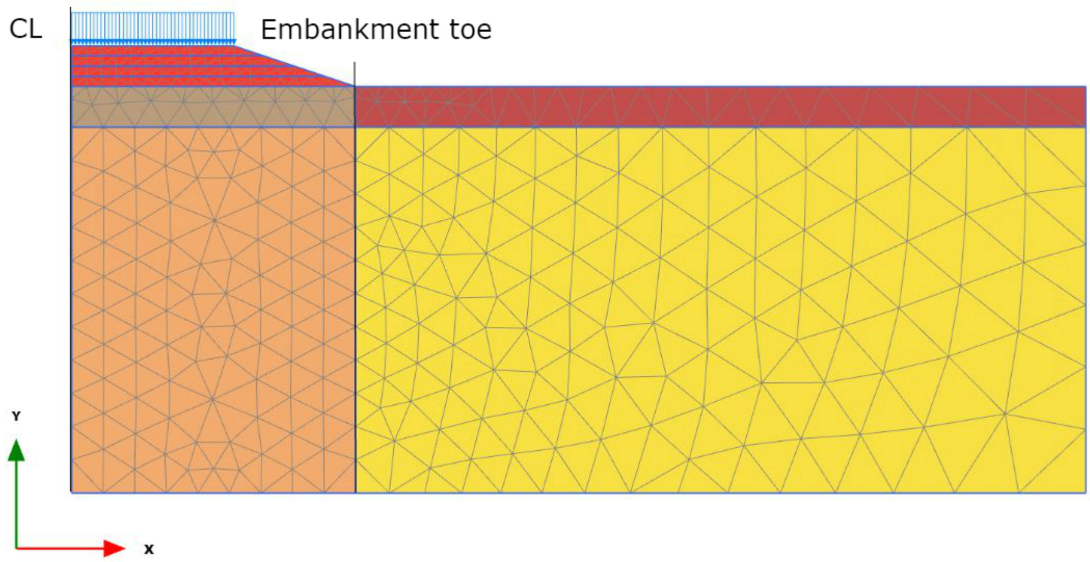

Figure 3.1: Problem geometry, soil layers and generated mesh.

3.3 Simulations cases

In this section the numerical investigations are described where same boundary value problem was simulated in both Geosuite Settlement and Creep-SCLAY1S. The centre line had a closed boundary for groundwater flow, combined with no horizontal displacements and the right boundary is fixed in same matter. The simulations was divided into three different cases, case I, case II and case III. Each case was analysed as a single- (SD) and double drainage (DD) condition. In Figure 3.2 the three cases are illustrated. The first case was simulated as a reference case without surcharge, sand layer and drains. In case II the full penetration length for the drains was kept and different amounts of surcharge was simulated. The last, case III, includes optimisation of the penetration length of the drains with the chosen optimal surcharge from case II.

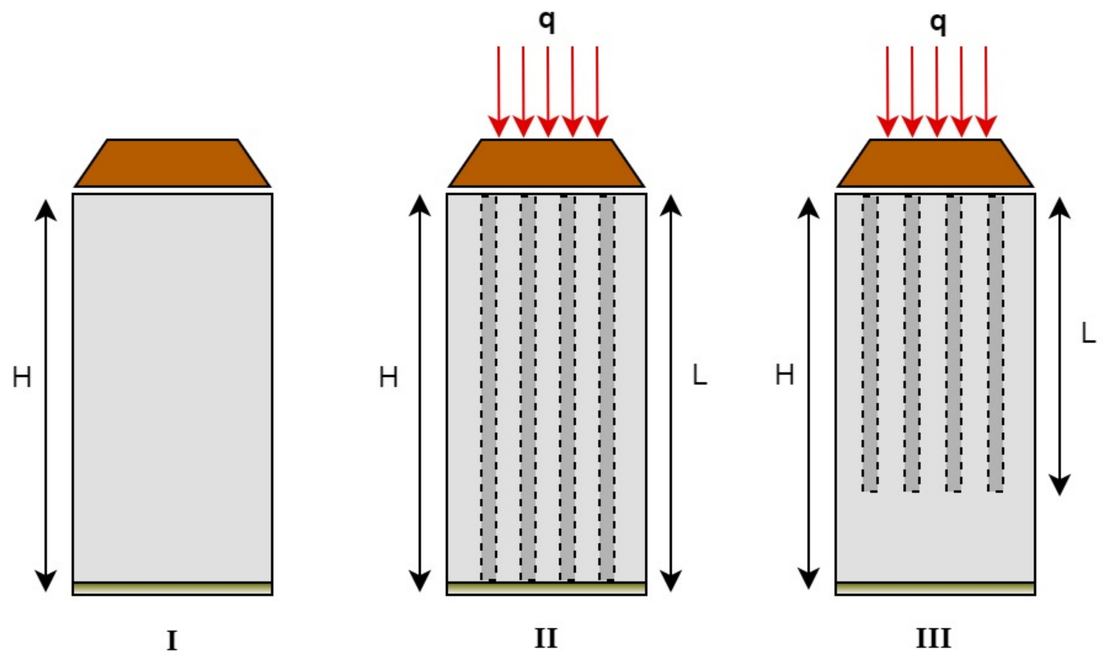

Figure 3.2: Illustration of the three different cases simulated.

3.4 Simulations with Geosuite Settlement

In Geosuite Settlement simulations was performed with the soil model called Chalmers with creep addendum, and the permeability model log based strain. The parameters were derived from the CRS-tests conducted from STII-piston samples. In Table 3.1 a summary of the parameters needed for Chalmersmodel with creep addendum is presented. The soil model used for the sand layer was Janbu-sand model. The parameters used for the sand was assumed to some reasonable values. In Appendix A.2 the parameters needed and used in Geosuite Settlement for the sand are presented. In Geosuite Settlement the embankment was simulated as a load and it was build instantly. On top of the embankment, various of surcharge loads was simulated. The surcharge load was consolidated for two years and then removed.

Division of the layers with respective parameters was set as illustrated in Table A.3. The unit weight of water was set as 10 kN/m^3 and the bulk modulus as 2×10^6 kN/m^2. The embankment was simulated as a constant line load and the surcharge is simulated in same matter. The tolerance factor that determines the range of error allowed was set as 0.0003 and maximum iteration per step was set to 1000.

Table 3.1: Parameters needed in Chalmersmodel with creep addendum.

Term in the model	*Unit*	*Explanation*
γ	kN/m^3	Unit weight of material
M_0	kN/m^2	Oedometer modulus at stress level > a_0 σ'_c
M_L	kN/m^2	Oedometer modulus at stress level between a_1 σ'_L
M'	-	Oedometer modulus at stress level < σ'_L
a_0	-	Stress factor ≥ 1
a_1	-	Stress factor ≤ 1
σ'_c	kN/m^2	Preconsolidation pressure
σ'_L	kN/m^2	Preconsolidation pressure
t_ref	*year*	Reference time, often assumed to be -1 day
b_0	-	Stress factor ≥ 1
b_1	-	Stress factor ≤ 1
r_0	-	Creep number at stress state b_0 σ'_c
r_1	-	Creep number at stress state b_1 σ'_c

3.5 Simulation with Creep-SCLAY1S model

The soil area below the embankment and sand layer represented the vertical drains. This area had a modified permeability during case II and III when the PVDs was active. Two types of PVDs were analysed, one set of floating PVDs and another one which covered the full depth of the soil. In order to perform the analysis in Plaxis 2D using Creep-SCLAY1S as a model, a total of 14 parameters are needed, and additional initial stress state parameters. As mentioned, Creep-SCLAY1S model takes into account the anisotropic, destructuration and viscous behaviour of the soil. The parameters used in this thesis have been derived and validated by Amavasai (2016). In Table 3.2, a summary of the parameters are presented and in Appendix A.4 the used parameters are presented.

Table 3.2: Parameters needed for Creep-SCLAY1S-model used in Plaxis 2D.

Parameter type	Parameter name	Parameter symbol
Isotropic	Modified swelling index	$\kappa*$
	Intrinsic compression index	$\lambda*_i$
	Poission's ratio	ν'
	Friction angle	ϕ'
	Stress ratio of critical state in compression	M_c
	Stress ratio of critical state in extension	M_e
Anisotropic	Initial inclination of yield stress	α_0
	Absolute effectiveness in rotational hardening	ω
	Relative effectiveness in rotational hardening	ω_d
Destructuration	Initial bonding	χ_0
	Absolute rate of degradation	ξ
	Relative rate of degradation	ξ_d
Viscous	Intrinsic creep coefficient	$\mu*_i$
	Reference time	τ_d
Initial stress	Unit weight of material	γ'
	Pre-consolidation pressure	σ'_c
	Lateral earth pressure at rest	K_0^{NC}
	Pre-overburden pressure	POP
	Over-consolidation ratio	OCR
	Initial void ratio	e_0

The initial phase introduced in the simulations of the embankment in Plaxis 2D is needed to represent the initial conditions in the field. The conditions needed to be analysed is the initial groundwater conditions and the initial effective stress state. The procedure is referred as the $K_0 - procedure$. After the initial phase the simulations continued with the embankment construction. The embankment was divided into four construction stages, where 0.5 meters was constructed within a time interval of three days until the final height was reached. After each embankment construction a consolidation phase of seven days was simulated, except from the last construction stage where the final consolidation stage took place. Different surcharge loads was placed on the embankment after finalisation of the embankment. After 399 days the surcharge load was removed, the embankment was left to consolidate for approximately 3000 years. In Table 3.3 the different simulations phases are presented.

Table 3.3: Staged construction as loading for the embankment.

No	*Stage of construction*	*Days*	*Calculation type*
1	Initial phase	(-)	K_o-procedure
2	0.5m embankment (+0.5m)	3	Consolidation
3	Consolidation	7	Consolidation
4	0.5m embankment (+1.0m)	3	Consolidation
5	Consolidation	7	Consolidation
6	0.5m embankment (+1.5m)	3	Consolidation
7	Consolidation	7	Consolidation
8	0.5m embankment (+2.0m)	3	Consolidation
9	Surcharge loading	1	Consolidation
10	Consolidation of surcharge	365	Consolidation
11	Consolidation	∞	Consolidation

4

Results

In this chapter simulation results combined with the discussion of the results for Geosuite Settlement and Creep-SCLAY1S are presented. The results follows the simulation cases described earlier in the methodology chapter, found in Section 3.3.

4.1 Simulation results from Geosuite Settlement

Figure 4.1 and 4.2 illustrates the results for single- and double drainage conditions for the different surcharge loads. In Geosuite Settlement the surcharge was unloaded after two years, and the expected swelling phenomena occurred. The reference simulation for SD shows that the EOP is not reached until 100 years, although that is not the case for the DD condition which reached EOP around 30 years. With ground improvements the single drainage condition reached EOP around 0.8 years, and for the double drainage it was reached around 0.2 years. The EOP occurred approximately four times faster for the double drainage condition compared to the single drainage condition, which is in line with the theory. The correlation is most probably due to that Geosuite Settlement is based on the one-dimensional consolidation theory proposed by Terzaghi (1923). In general the settlements after EOP are low, between 1-100 years the pure creep settlements was approximately 15 cm for DD and 10 cm for SD. The low settlements follows the low creep rates from the simulation results. The low creep rates are in line with Leoni et al. (2008), which stated that higher OCR than 1.3 had negligible creep rates. The figures also indicates unreasonably high swelling at higher AAOS. It is important to bear in mind that Geosuite Settlement is based on Hypothesis A where creep does not occurs simultaneously with the primary consolidation. Models based on Hypothesis A will have a significant reduction of the total settlements since the contribution of creep will start after EOP.

The creep evaluation for these simulations was performed with out any modification of the original method presented by Ladd (1971). The results obtained from the creep evaluation are presented in Figure 4.3. From Figure 4.3, it is evident that none of the drainage conditions correlates with Ladd's mean line. The results from SD and DD-drainage shows significantly lower creep improvement ratios compared to

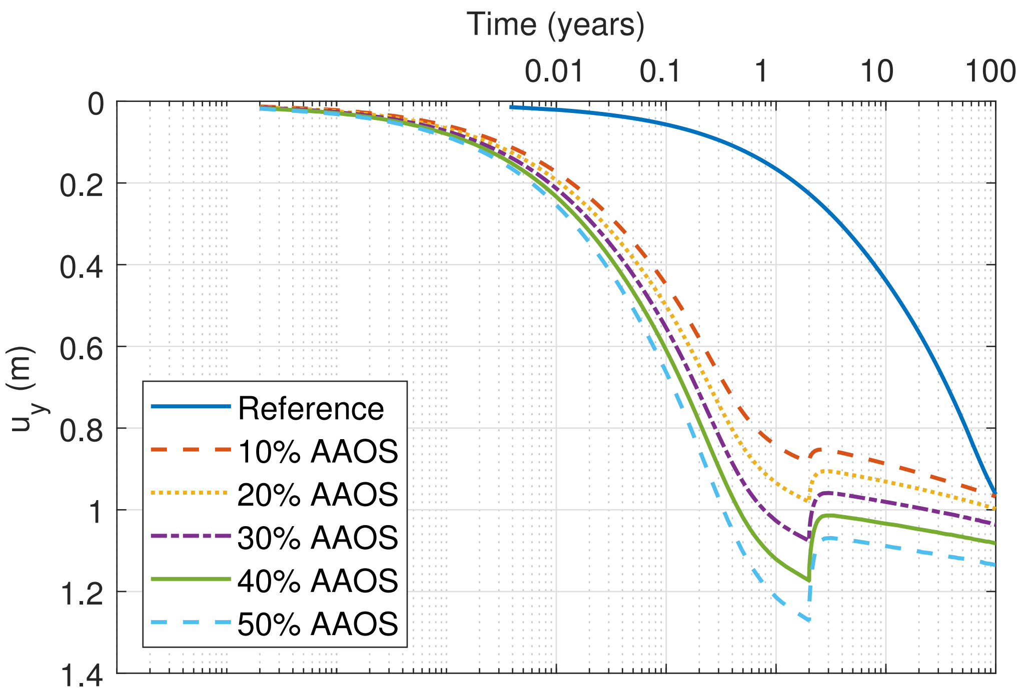

Figure 4.1: Case II with unloading of AAOS after 2 year. Single drainage with PVDs at full penetration length.

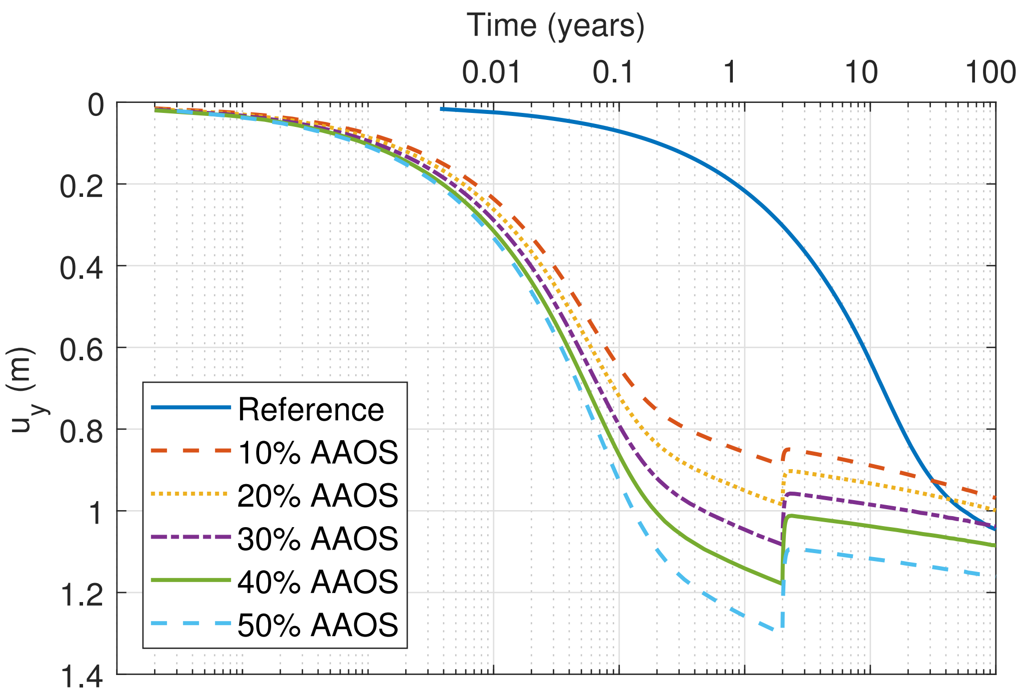

Figure 4.2: Case II with unloading of AAOS after 2 year. Double drainage with PVDs at full penetration length.

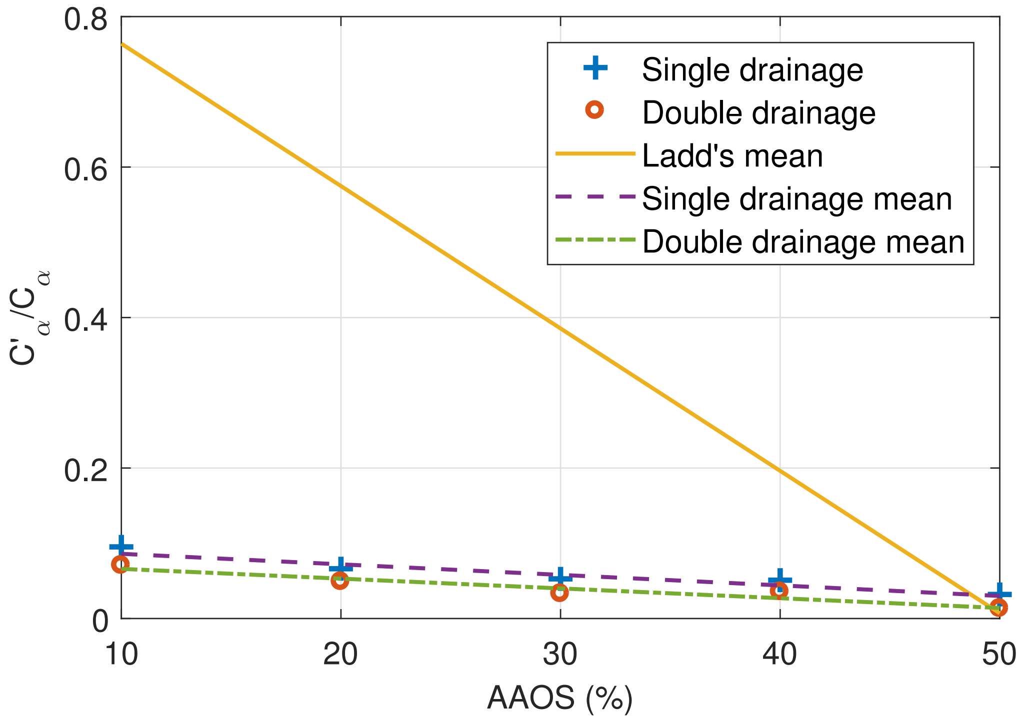

Figure 4.3: Creep improvement ratio due to surcharge, derived from both drainage conditions in case II using the method proposed by Ladd (1971).

Ladd's mean line. This implies that the creep rates are expected to be lower during the embankments life time according to this analysis. Comparing the two drainage conditions, it can be seen that slightly lower creep improvement ratios are expected for double drainage condition, although, the results indicates that increasing AAOS will not necessarily produce lower creep rate. Another reason could be that soils with an OCR-value equal or higher than 1.3 has negligible creep rates as stated by Leoni et al. (2008), producing low creep improvement ratios.

The analysis from case II in Geosuite Settlement indicated similar results as in Creep-SCLAY1S. The penetration depth of the PVDs (case III) was also optimised with 20% AAOS. The results for case III are illustrated in Figure 4.4 and 4.5. Vertical displacements at centre line of the embankment are plotted against the time for different penetration depths. The results for single drainage conditions point outs that penetration depth between L/H=0.3-0.8 has an impact on end of primary consolidation, thus the drain length could be reduced by 10% (L/H=0.9). Although, for double drainage the length of the PVDs could be reduced by 20% (L/H=0.8) without affecting end of primary consolidation. These results are in well accordance with results presented in Ikhya and Schweiger (2012), where drain length could be reduced by 20% for the double drainage, and 10% for the single drainage condition.

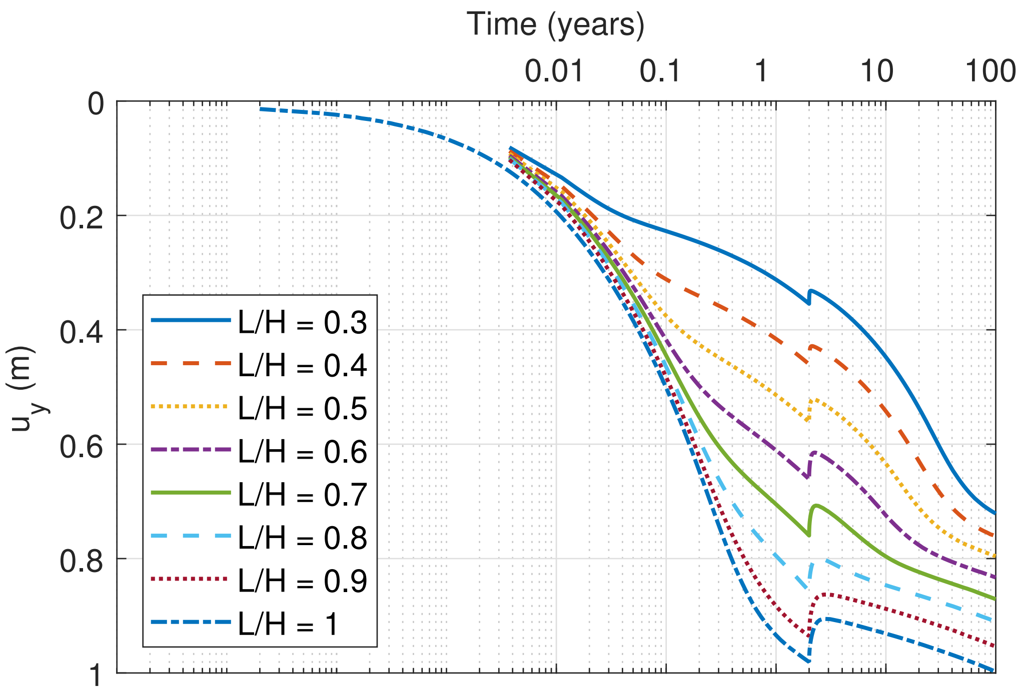

Figure 4.4: Optimisation of penetration length of the PVDs for single drainage.

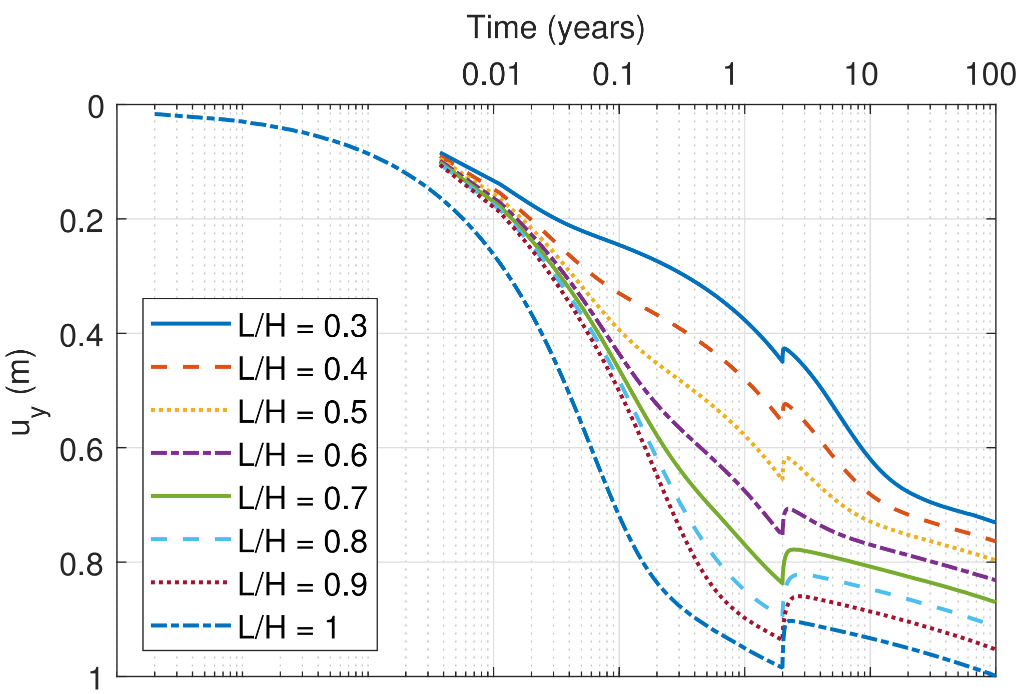

Figure 4.5: Optimisation of penetration length of the PVDs for double drainage.

4.2 Simulation results from Creep-SCLAY1S

The first simulations were simulated to establish the reference cases for single (SD)- and double drainage (DD) conditions respectively. Case I is presented in Figure 4.6, consisting of single- and double drainage, with and without prefabricated vertical drains (PVDs). SD and DD without PVDs has an end of primary consolidation (EOP) after approximately 100 and 300 years, respectively. In theory the double drainage condition should reach EOP four times faster than the single drainage condition. In contrast, primary consolidation ends after approximately one year for both drainage conditions with PVDs. After 100 years the embankment with PVDs is predicted to settle up to two meters, resulting in equal level as the initial ground surface. PVDs significantly improves the EOP and a large share of the total settlements has already occurred after one to three years. For the conditions without PVDs, large post construction settlements starts to occur after one year. Without ground improvement that serviceability during the embankments life time (40 years) is most likely affected.

Another interesting aspect is that for the SD condition without PVDs high creep rates are produced. This is suggesting that even after 1000 years primary and secondary consolidation is on-going. In general, better drainage conditions contributes to larger total settlements of the soil. The double drainage condition had a small improvement on the EOP when PVDs at full depth was activated. The small difference in EOP for the drainage conditions is probably due to the performance of the drains. The change of improved clay layer acting as drains had high enough permeability, which made the drainage condition insignificant. Even in the case without ground improvements the double drainage conditions did not reach four times faster EOP. This due to that the boundary value problem in this study had different conditions compared to the ones mentioned earlier in the theory Section 2.1.

Figure 4.7 and 4.8 illustrates the optimisation results of different surcharge loads for the SD and DD conditions. The results indicates that a higher percentage of adjusted amount of surcharge (AAOS) reduces the time for EOP and this because a higher pore water pressure gradient increase the rate of consolidation. Comparing the two drainage conditions it was noticed that EOP was occurring earlier for the DD condition. Analysing the simulations done at 10% AAOS for both types of drainage conditions, it was proven that EOP for SD was reached after approximately three years whereas for the DD the EOP ended after approximately one year. Surprisingly, no swelling is predicted after unloading at various AAOS for both conditions. A single simulation was performed where the load was left in place for a longer time and with a higher load than 50% AAOS, still no swelling occurred. This is suggesting that the intrinsic creep rates could be higher than any predicted swelling. This could be due to the Creep-SCLAY1S model does not properly capture the swelling phenomena after unloading. Another reason may be that the Creep-SCLAY1S model is based on Hypothesis B which was mentioned in Section 2.2, producing such extensive settlements that even a swelling of small magnitude may remain unnoticed. One simulation, not presented in these results, was done in the Soft Soil Creep model,

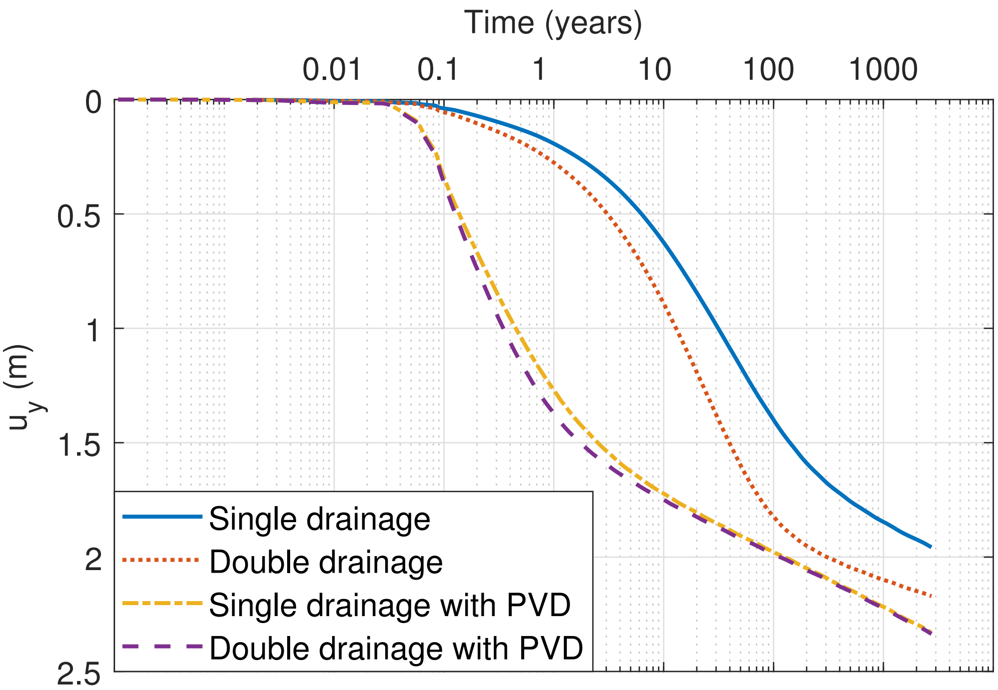

Figure 4.6: Results from case I, single- and double drainage conditions with and without PVDs.

available in Plaxis 2D. The results proved that no swelling was found there either. This could indicate that there are issues with the fundamental model formulation. Another interesting aspect is that this issues could address to evaluation of modified swelling index ($\kappa*$) and intrinsic creep coefficient (μ_i^*) from the laboratory tests.

In Leoni et al. (2008) it was stated that soil with OCR-value of 1.3 and more had negligible creep rates. The Creep-SCLAY1S model verified the opposite. Figure 4.7 and 4.8 illustrates that the both drainage conditions had high creep rates. Between the time interval 1-100 years, settlements amounted to approximately 0.6 meter for 10% AAOS, and increasingly with higher AAOS.

One of the issues that emerged from the findings in case II was the difficulties with evaluation of the creep rates before and after swelling. The swelling is critical in order to visualise when and if the creep improvement occurs after unloading. Therefore, the evaluation of creep improvement had to be modified for the Creep-SCLAY1S results. The evaluation of the creep rates was done by plotting the creep improvement ratio C'_α/C_α versus the various AAOS as presented in Ladd (1971). The creep rate C_α was derived from simulations done in case I, both drainage cases were then used as a reference. The improved creep rate C'_α was then compared for each drainage condition respectively. Creep rates was analysed after 1300 years. The results for improved creep rates after 1300 years are illustrated in Figure 4.9. The results indicate that higher percentage of AAOS results into lower creep improvement ratios and lower creep rates. These results need to be interpreted with caution since they

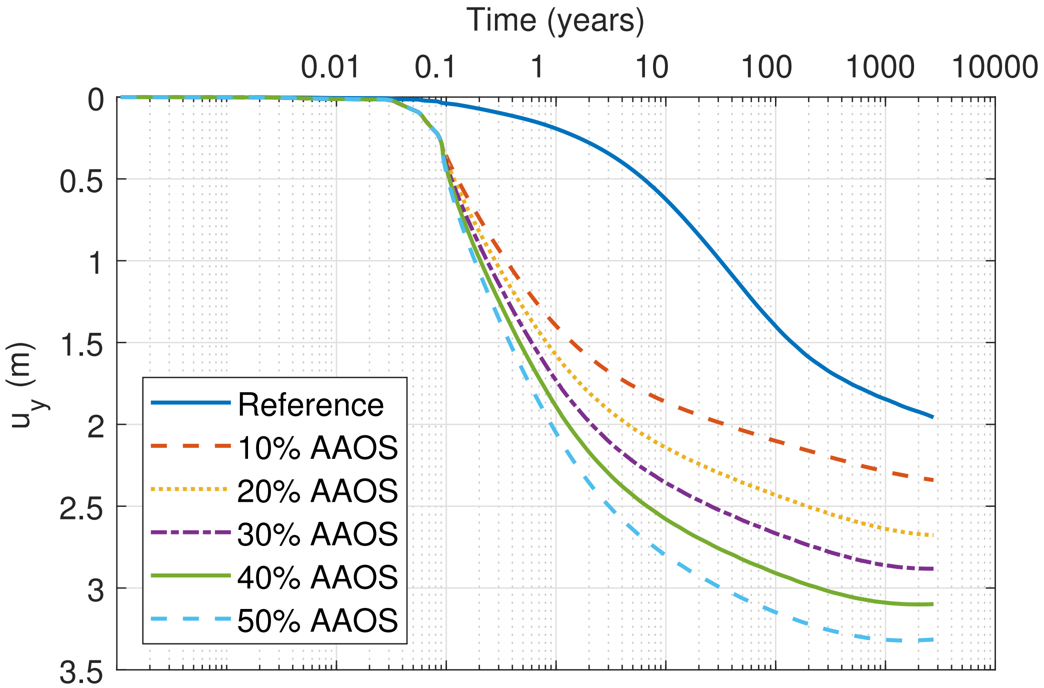

Figure 4.7: Case II with unloading of AAOS after 1 year. Single drainage with PVDs at full penetration length.

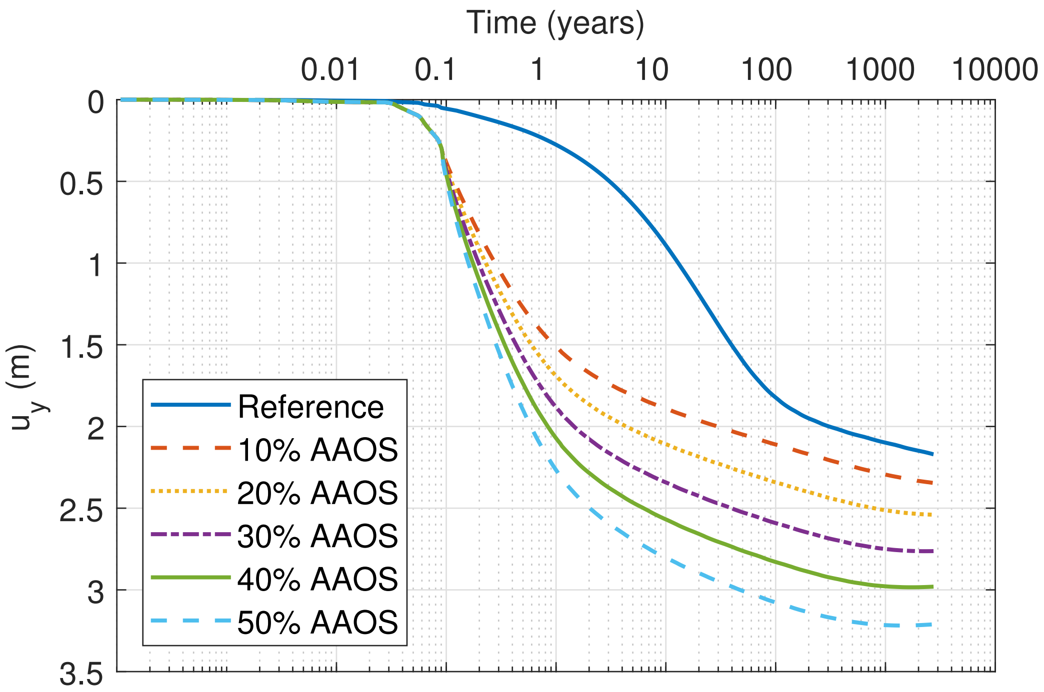

Figure 4.8: Case II with unloading of AAOS after 1 year. Double drainage with PVDs at full penetration length.

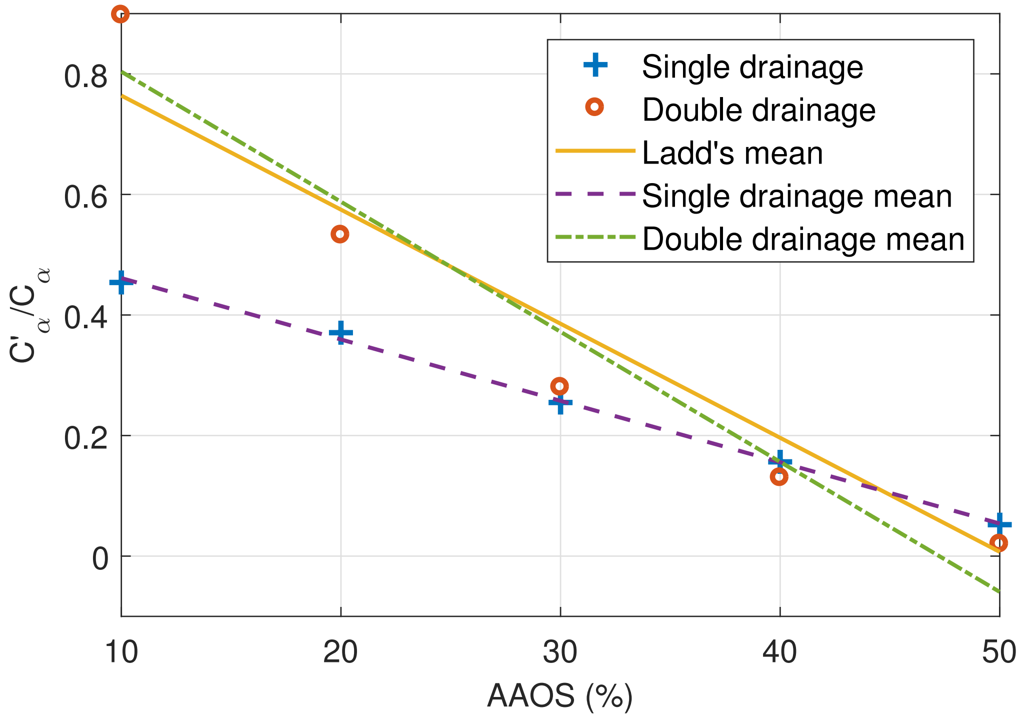

Figure 4.9: Creep improvement ratio due to surcharge, derived from both drainage conditions in case II after 1300 years.

only occur around 1300 years. Performing the same evaluation for another time frame would produce different results. However, the results for double drainage condition supports the procedure presented by Ladd (1971) that mimics the typical loading regime for embankment constructions. The results for single drainage also indicates the expected behaviour, although the reduction of creep rate seems to be lower with the incremental of AAOS.

In Figure 4.10 and 4.11 horizontal displacements are presented for both drainage conditions. The figures shows horizontal displacements versus soil depth, and are normalised with the embankment height. Analysing the both conditions, no significant difference was noted between the SD and DD-conditions. The horizontal displacements was affected by varying magnitude of the AAOS, similar to the results for the vertical displacements. These results suggests that larger horizontal displacements occurs at higher AAOS. At 50% AAOS the displacements are high enough to affect up to 30 cm at each side of the embankment. Although, these displacements are fully developed after approximately 2700 years.

After the simulations with different AAOS was finished, the analysis proceeded with the optimisation of the penetration depth (case III). This case was optimised with the surcharge load 8 kPa which is equal to 20% AAOS. This surcharge load was chosen since higher loads gave excessively large settlements, lower loads seemed unreasonably low for a two meter high embankment construction. In Figure 4.12 and 4.13 the vertical displacements depth against time are plotted for different penetration

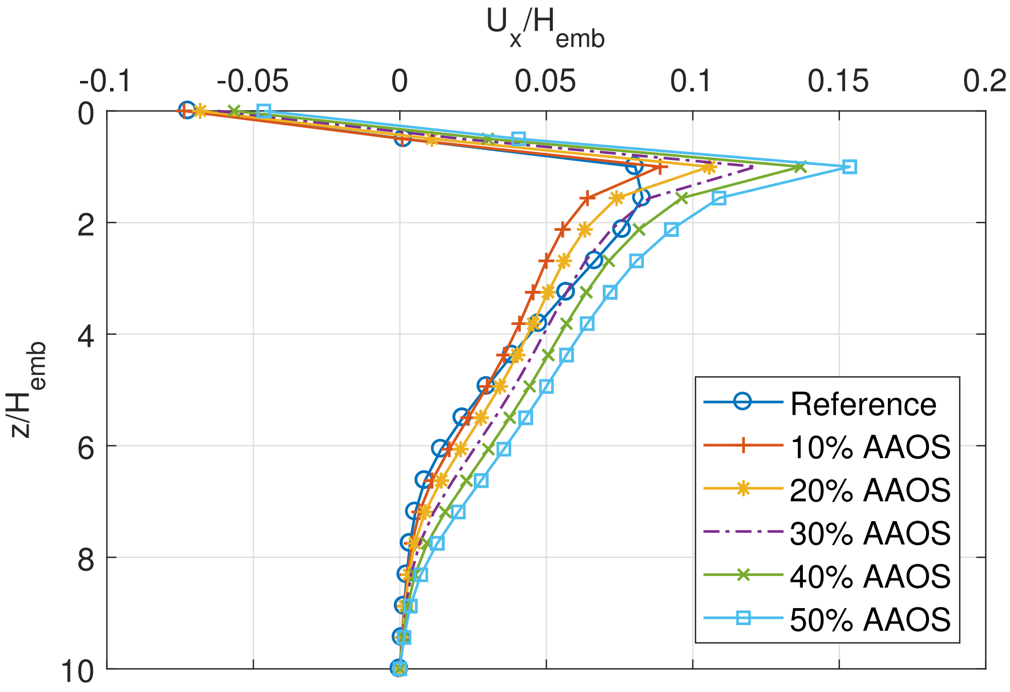

Figure 4.10: Horizontal displacements at embankment toe for different AAOS, case II for SD conditions.

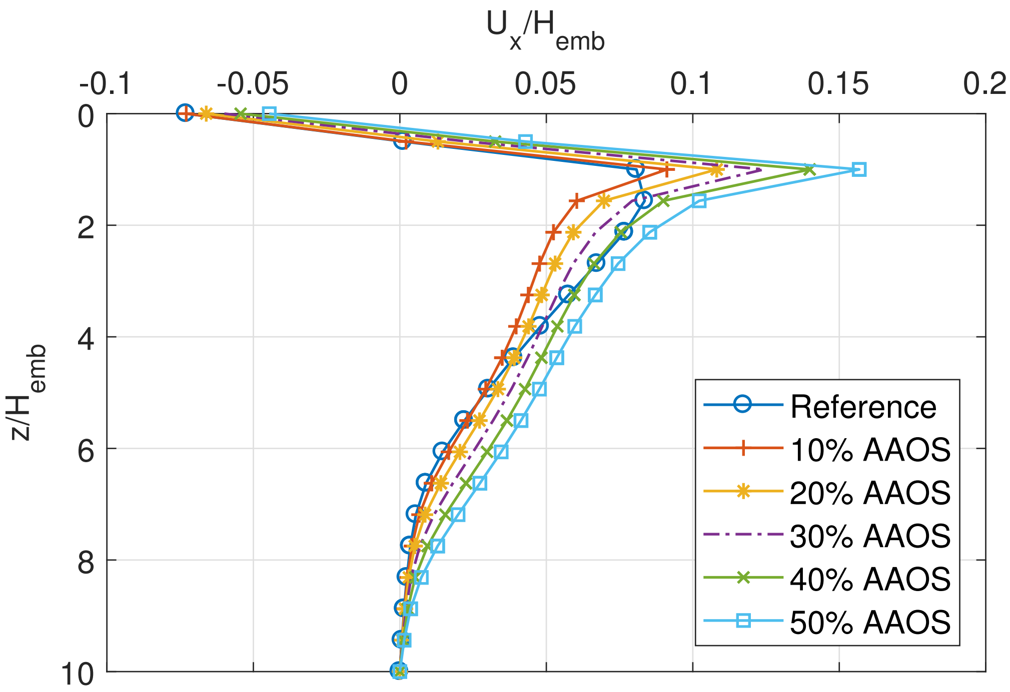

Figure 4.11: Horizontal displacements at embankment toe for different AAOS, case II for DD conditions.

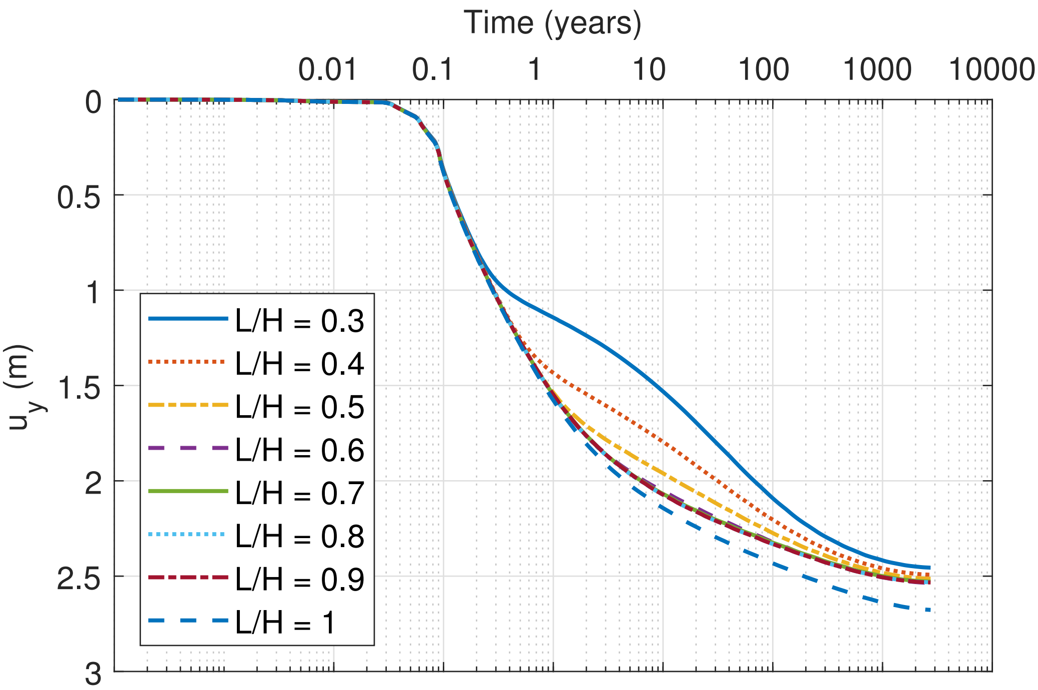

Figure 4.12: Optimisation of penetration length for single drainage.

depths. The figures indicate that the penetration depths of 0.3-0.5 for both drainage conditions affects the EOP, resulting in prolonging the time needed for primary consolidation to end. Further on, the analysis showed that the penetration depth could be reduced up to L/H=0.6 without affecting the consolidation process. These results are in agreement with those obtained by Indraratna and Rujikiatkamjorn (2008), which concluded that the drain length can be reduced with 40%. The length of the PVDs could even be reduced up 50% which slightly influences the consolidation process. However, these results is contrary to that of Geng et al. (2011), where it was concluded that the length of PVDs in general can be reduced with 20% to achieve a normalised settlement of 90%. Ikhya and Schweiger (2012) found that the drain length for a homogeneous soil could be reduced up to 20% for double drainage and only 10% for single drainage, without significantly affecting the consolidation process. These results together provide important insights into how deep the drains should be installed at ground improvements.

Figure 4.14 and 4.15 presents the results for horizontal displacements for different penetration lengths of the PVDs. In the figures depth of the soil versus the horizontal displacements is plotted, and both axes are normalised with the embankment height. Analysing the results from the figures no significant difference was noted between the two drainage conditions. Lower penetration depths than 50% shows most deviations from the deeper penetration lengths. There was a significant positive correlation between the results from this study with Indraratna and Rujikiatkamjorn (2008) considering the lateral displacements. In Indraratna and Rujikiatkamjorn (2008) it can be seen that no distinguishable difference was noticed for the horizon-

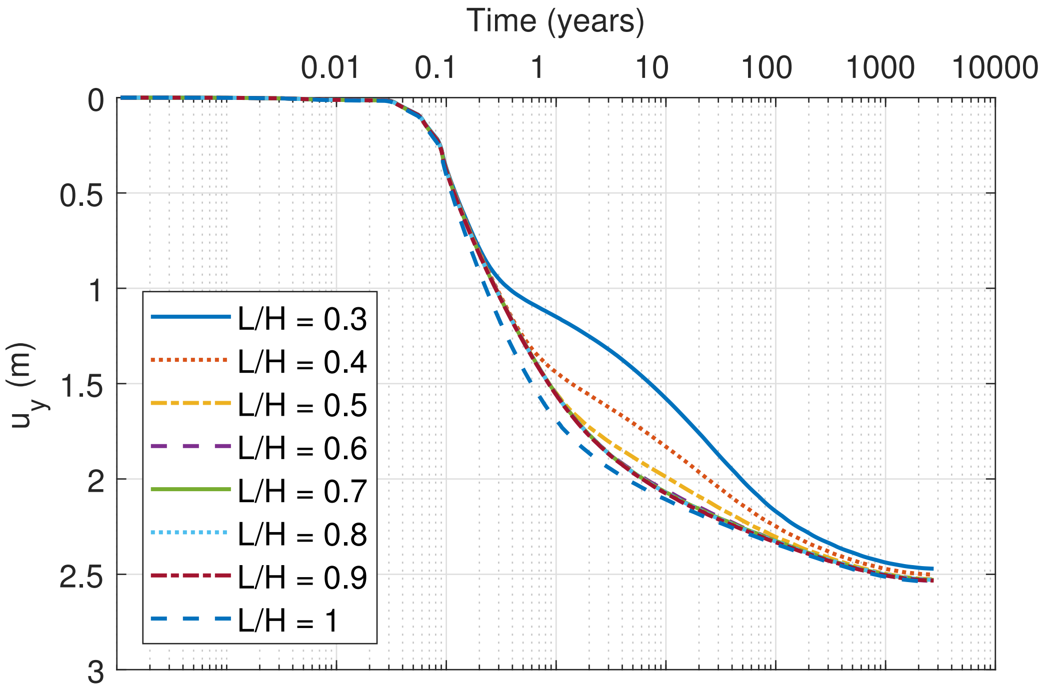

Figure 4.13: Optimisation of penetration length for double drainage.

tal displacements when reduction of the PVDs are in the range L/H=1-0.5. However, the simulations in this study are extended to even lower penetration depths than 50%. The lower penetration depths shows a deviating trend, resulting in larger horizontal displacements between the range $z/H_{emb} = 2 - 5$.

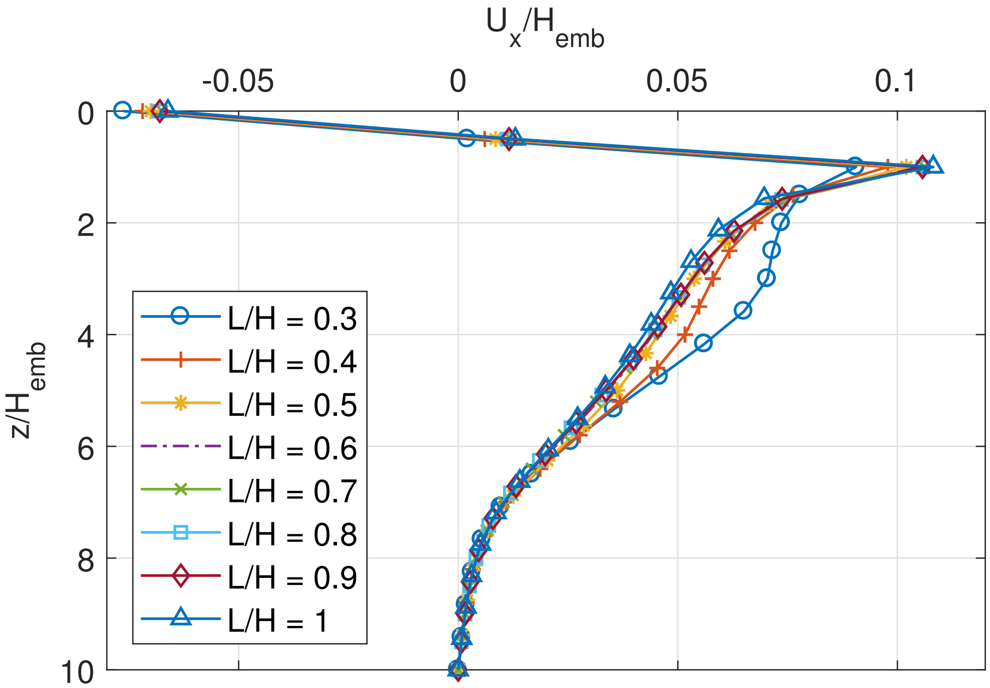

Figure 4.14: Horizontal displacements at embankment toe for single drainage when optimising penetration length of the PVDs.

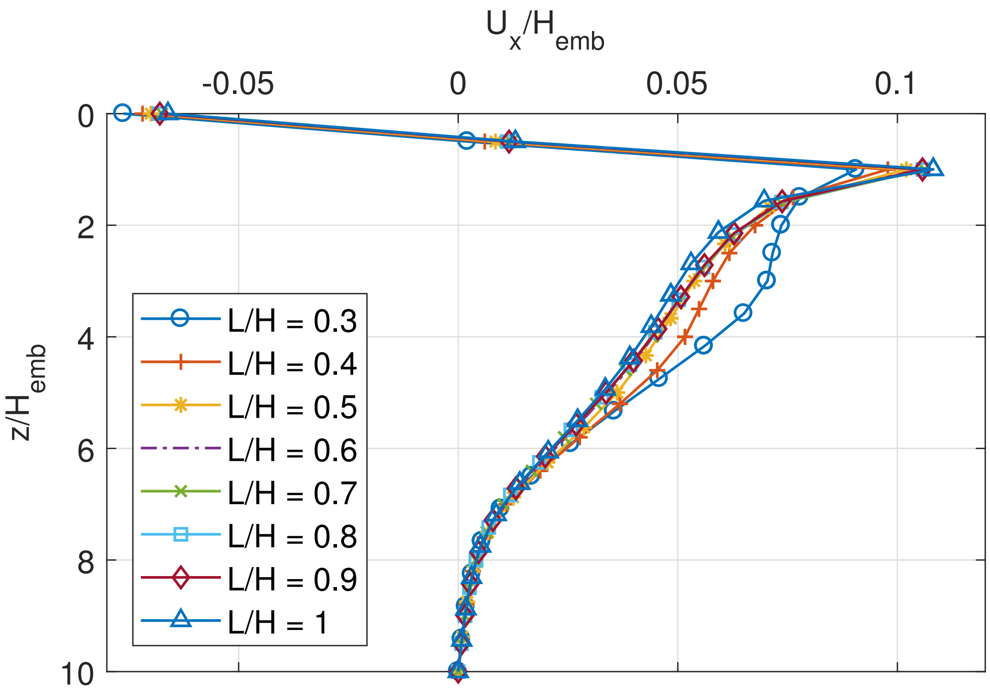

Figure 4.15: Horizontal displacements at embankment toe for double drainage when optimising penetration length of the PVDs.

5

Conclusion

The aim of the present research was to examine if creep could be eliminated or reduced with the support of ground improvement. Numerical modelling was assessed to analyse three different cases in Geosuite Settlement and Plaxis 2D. This in order to find the optimal design of the surcharge load and prefabricated vertical drains.

The study has shown that Geosuite Settlement captures the swelling phenomena. The swelling occurred instantly and for higher loads it amounted up to 10 cm, which seems unreasonable. The evaluation of creep improvement ratio showed that the results were not in line with Ladd (1971) proposal of mean line. However, the results from Geosuite Settlement implies that if higher AAOS is applied, the higher reduction of creep rate after unloading. High magnitude of AAOS should be applied with caution, since these produce excessive settlements which may affect the constructions serviceability. The evaluated results for optimisation of penetration length shows that the penetration depth could be reduced up to 10% for single drainage condition without significantly affecting the consolidation process. On the other hand, for the double drainage condition, penetration depth could be reduced by 20% without significantly affecting EOP.

This study has also identified that Creep-SCLAY1S does not capture the swelling phenomena properly. In general, the model predicts excessive settlements, where secondary compression amounts up to approximately 30 percent of the total settlements. From the optimisation results, it can be concluded that increasing AAOS will not necessarily improve the creep rates, although, after 1300 years it is evident that creep rates was significantly improved by higher AAOS. Even here caution should be taken regarding the high surcharge loads contributing to excessive settlements. The optimisation results also proves that the penetration length of the prefabricated vertical drains could be reduced up to 40% without affecting the consolidation process, which is valid for the single and double drainage conditions.

A limitation of this study is that no swelling was noted in the Creep-SCLAY1S simulations. Therefore, the method proposed by Ladd (1971) had to be modified. Even when the modification was done, the results indicated that creep rates could not be improved within the scope of practical applications. Results from Geosuite Settlement enabled using the method proposed by Ladd (1971) and it could be concluded that creep could not be eliminated, although significant reduced creep rates was achieved.

Further work should focus on investigating the model formulations for the Soft Soil Creep and Creep-SCLAY1S models. The works should look into the the swelling which has passed unnoticed in this study. One suggested approach is to perform a sensitivity analysis of the modified swelling index ($\kappa*$) and intrinsic creep coefficient ($\lambda*_i$). Additionally, if a similar study is made, embankments with available long-term field measurements should be included in the analysis.

Bibliography

Alm, L.-O. (2000). *Course Compendium, Road and Street Design.*

Almeida, M. and Marques, E. (2013). *Design and Performance of Embankments on Very Soft Soils.* CRC Press.

Alén, C. (1998). *On probability in geotechnics.* PhD thesis, Chalmers University of Technology.

Amavasai, A. (2016). Parameter derivation and its validation for creep-sclay1s model from utby samples. Technical report, Deparment of Geotechnical Engineering of Chalmers Technical University, Gothenburg.

Balasubramaniam, A. S., Cai, H., Zhu, D., Surarak, C., and Oh, E. Y. N. (2010). Settlements of embankments in soft soils. *Geotechnical Engineering Journal of the SEAGS & AGSSEA.*

Brand, E. W. and Brenner, R. P. (1981). *Soft Clay Engineering.* ELSEVIER SCIENTIFIC PUBLISHING COMPANY.

Chai, J.-C., Shen, S.-L., Miura, N., and Bergado, D. T. (2001). Simple method of modeling pvd-improved subsoil. *Journal of Geotechnical and Geoenvironmental Engineering*, 127.

Claesson, P. (2003). *Long term settlements in soft clays.* PhD thesis, Chalmers University of Technology.

Conroy, T., Fahey, D., Buggy, F., and Long, M. (2015). Control of secondary creep in soft alluvium soil using surcharge loading. Technical report, University College Dublin.

Fatahi, B., Lê, M., and Khabbaz, H. (2013). Soil creep effects on ground lateral deformation and pore water pressure under embankments. *Geomechanics and Geoengineering.* DOI: 10.1080/17486025.2012.727037.

Geng, X., Indraratna, B., and Rujikiatkamjorn, C. (2011). Effectiveness of partially penetrating vertical drains under a combined surcharge and vacuum preloading. *Canadian Geotechnical Journal*, 48(6):970–983.

Gras, J.-P., Sivasithamparam, N., Karstrunen, M., and Dijkstra, J. (2015). Permissible range of model parameters for natural fine-grained materials. *Acta Geotechnica.* DOI: 10.1007/s11440-017-0553-1.

Grimstad, G., Degago, A. S., Nordal, S., and Karstunen, M. (2010). Modeling creep and rate effects in structured anisotropic soft clays. *Acta Geotechnica.* DOI: 10.1007/s11440-010-0119-y.

Hansbo, S. (1981). Consolidation of fine-grained soils by prefabricated drains. *In Proceedings of the 10th International Conference on Soil Mechanics and Foundation Engineering, Stockholm, Edited by Publications Committee of the ICSMFE. A.A. Balkema, Rotterdam, The Netherlands*, 3:677–682.

Ikhya, I. and Schweiger, H. (2012). Numerical modelling of floating prefabricated vertical drains in layered soil. *Acta Geotechnica Slovenica.*

Indraratna, B. and Rujikiatkamjorn, C. (2008). Effects of partially penetrating prefabricated vertical drains and loading patterns on vacuum. *University of Wollongong.* http://dx.doi.org/10.1061/40971(310)74.

Kalmykova, Y., Rosado, L., and Patrício, J. (2015). Resource consumption drivers and pathways to reduction: economy, policy and lifestyle impact on material flows at the national and urban scale. *Journal of Cleaner Production*, pages 1–11. http://dx.doi.org/10.1016/j.jclepro.2015.02.027.

Karlsson, M., Emdal, A., and Dijkstra, J. (2016). *Consequences of sample disturbance when predicting long-term settlements in soft clay.* Chalmers University of Technoligy.

Karstunen, M., Sivasithamparam, N., Bringreve, R., and Bonnier, P. (2013). Modelling rate-dependent behaviour of structured clays. In *International Conference on Installation Effects in Geotechnical Engineering (ICIEGE)*, pages 43–50.

Kirsch, K. and Bell, A. (2013). *Ground Improvement.* Spon Press.

Knappett, J. and Craig, R. (2012). *Craig's Soil Mechanics.* Spon Press, 8 edition.

Ladd, C. C. (1971). Settlement analyses of cohesive soils. Technical report, Department of Civil Engineering, M.I.T., Canbridge, Massachusetts.

Ladd, C. C., Foott, R., Ishihara, K., Schlosser, K., and Poulos, H. G. (1977). Stress-deformation and strength characteristics. state-of-the-art report. *Géotechnique*, page 421–494. DOI 10.1680/geot.2001.51.10.859.

Leoni, M., Karstunen, M., and Vermer, P. (2008). Anisotropic creep model for soft soils. *Geotechnique*, 58:215–226. http://dx.doi.org/10.1680/geot.2008.58.3.215.

Mehner, H. (2017). Urban development in gothenburg. http://goo.gl/Lm8mF3.

Mesri, G. and Funk, J. R. (2015). Settlement of the kansai international airport islands. *Journal of Geotechnical and Geoenvironmental Engineering*, 14. http://dx.doi.org/10.1061/(ASCE)GT.1943-5606.0001224#sthash.uPpp9Lfr.dpuf.

Mitchell, J. K. and Soga, K. (2005). *Fundamentals of Soil Behavior*. John Wiley & Sons, Inc., Hoboken, New Jersey, 3 edition.

Navarro, V. and Alonso, E. E. (2001). Secondary compression of clays as a local dehydration process. *Géotechnique*, page 859–869. DOI 10.1680/geot.2001.51.10.859.

Puzrin, Alonso, and Pinyol (2010). *Geomechanics of Failures*. Springer Netherlands.

Sivasithamparam, N., Karstrunen, M., and Bonnier, P. (2015). Modelling creep behaviour of anisotropic soft soils. *Computers and Geotechnics 69*, 3:1–12. http://dx.doi.org/10.1016/j.compgeo.2015.04.015.

Swedish Standard Institute, S. (1991). Geotekniska provningsmetoder – kompressionsegenskaper – Ödometerförsök. crs-försök – kohesionsjord. *Geoteknik och geokonstruktioner, SIS/TK 183*.

Swillingand, M. and Robinson, B. (2013). Urban resource flows and the governance of infrastructure transitions. *Environmental Development*, pages 152–153. `http://dx.doi.org/10.1016/j.envdev.2013.09.002`.

Terzaghi, K. (1923). *Die Berechung der Durchlässigkeitsziffer des Tones aus dem Verlauf der hydrodynamishe Spannungserscheinungen.*, volume 132. John Wiley and Sons, Inc.

Terzaghi, K. (1943). *Theoretical Soil Mechanics*. John Wiley and Sons, Inc.

Tewatia, S. K., Bose, P. R., Sridharan, A., and Rath, S. (2007). Stress induced time dependent behavior of clayey soils. *Geotechnical and Geological Engineering*, page 239–255. DOI 10.1007/s10706-006-9107-2.

Wheeler, S. J., Näätänen, A., Karstunen, M., and Lojander, M. (2003). An anisotropic elastoplastic model for soft clays. *Canadian Geotechnical Journal*, pages 403–418.

A

Appendix

A.1 Derivation of improved permeability (k_{eq})

Table A.1: Calculation of improved permeability to represent the PVDs in the soil.

Parameters	value	Unit
c_v	3.15	m^2/yr
c_h	4.0	m^2/yr
t	t	yr
k_h	1×10^{-9}	m/s
k_s	2.5×10^{-10}	m/s
d_s	0.53	m
d_w	0.07	m
$U_{v,h}$	0.9	%
T_v	0.03	$-$
U_v	0.27	%
U_r	0.88	%
s	8	$-$
S	2	m
D	2.26	m
T_r	0.2	$-$
n	34.18	$-$
μ	9.02	$-$
U_r	0.16	$-$
q_w	4.8×10^{-6}	m^3/s
k_{ev}	1.4×10^{-6}	m/s
k_{ev}	1.4×10^{-2}	m/day

A.2 Parameters needed for Chalmersmodel

A summary of the parameters needed to use Chalmersmodel with the creep addendum in Geosuite Settlement and Janbu-sand model.

Table A.2: Parameters needed for sand layer using Janbu-sand model.

Sand layer	ρ (kg/m^3)	m $(-)$	a $(-)$	r_m	σ'_c (kPa)	$k_{initial}$ (m/yr)	β_k $(-)$
0-2 m	18	200	0.5	1.0	46.8	0.5	1.0

Table A.3: Model parameters the clay layer using Chalmersmodel with creep addendum.

Soil layer	2-20 m
ρ (kg/m^3)	14.8
M_0 (kN/m^2)	1415
M_L (kN/m^2)	207
M' $(-)$	8.3
a_o $(-)$	0.8
a_1 $(-)$	1.0
σ'_c (kPa)	76
σ'_L (kPa)	90
t_{ref} (day)	-1
b_0 $(-)$	0.76
b_1 $(-)$	1.1
r_0 $(-)$	754.30
r_1 $(-)$	80.62
k_{intial} (m/s)	$1.04 \cdot 10^{-9}$
β_k $(-)$	0

A.3 Denotation of creep number, r

Below, equation for denoting the creep addendum parameters are presented.

$$r_1 = \frac{75}{w_N^{1.5}} \tag{A.1}$$

where w_N is the natural water content in the soil.

$$r_0 = \psi \cdot (b_1 - b_0) + r_1 \tag{A.2}$$

where the constant ψ determines the rate of creep. Usually, the constant ψ is set between 2000-3000. If large creep rate is desired low values are set and vice verse.

$$b_0 = \frac{\sigma_0'}{\sigma_c'} \tag{A.3}$$

In table A.4, the calculated creep addendum parameters for Chalmersmodel are presented.

Table A.4: Calculated parameters for Chalmersmodel with creep addendum.

Term	*Unit*	*Clay layer*
r_1	–	80.62
ψ	–	2000
w_N	%	95.3
r_0	–	754.30
b_0	–	0.76
b_1	–	1.1
σ_0'	kN/m^2	58
σ_c'	kN/m^2	76

A.4 Parameters needed for Creep-SCLAY1S

In the following tables, parameters used to simulate the boundary value problem with Creep-SCLAY1S model are presented and derived by Amavasai (2016).

The additional initial stress state parameters for the soil layers.

Table A.5: The additional initial stress state parameters for the soil layers.

$Material$ $(-)$	$Model$ $(-)$	ρ (kg/m^3)	E (MPa)	v $(-)$	K_0 $(-)$	φ' $(°)$	c' (kPa)
Embankment	MC	2.0	25	0.3	1	35	2
Sand	MC	1.8	5	0.3	0.5	30	5
Dry crust	MC	1.8	7	0.3	0.7	30	1
Clay	Creep-SCLAY1S	1.55	1	1	1	30	N/A

Table A.6: Isotropic parameters used for the clay layer.

$Isotropic\ parameters$ $(-)$	κ^* $(-)$	λ_i^* $(-)$	v $(-)$	M_c $(-)$	M_e $(-)$	φ' $(°)$
Clay	0.01	0.122	0.18	1.075	0.79	30

Table A.7: Anisotropic parameters used for the clay layer.

$Anisotropic\ parameters$ $(-)$	α_0 $(-)$	ω $(-)$	ω_d $(-)$
Clay	0.4125	30	0.6067

Table A.8: Destructuration parameters used for the clay layer.

$Destructuration\ parameters$ $(-)$	χ_0 $(-)$	ξ $(-)$	ξ_d $(-)$
Clay	5.08	9	0.2

Table A.9: Viscous parameters used for the clay layer.

$Viscous\ parameters$ $(-)$	μ_i^* $(-)$	τ $(days)$
Clay	0.0013	1